Course Booklet

Units 2 & 3

Version 1,0

May 19, 2021

DARA Course Booklet
Unit 2 and 3

Version 1.0

May 19, 2021

Welcome

Welcome to the Development of African Radio Astronomy training school. This document consists of an overview of different subject materials that will be covered in your time on site covering DARA units 2 and 3. Alongside the lecture notes will be some exercises that will help with your course material. The syllabus content is as follows:

- Introduction to Radio Astronomy
- Receivers
- Backends & DSP
- Coordinate Systems
- Timing Systems
- Pulsars
- Interferometry
- Very Long Baseline Interferometry
- Astrometry
- Fourier Transforms
- Single Dish Astronomy
- Radio Frequency Interference
- Spectroscopy
- Telescope Proposal Writing
- Calibration

Contents

Glossary

This glossary contains a list of words, terms and acronyms that you will come across in Radio Astronomy.

UTC - Coordinated Universal Time

GMST - Greenwich Mean Sidereal Time

LNA - Low Noise Amplifier

RFI - Radio Frequency Interference

IF - Intermediate Frequency

RF - Radio Frequency

DSP - Digital Signal Processing

VNA - Vector Network Analyser

Coaxial cable - A transmission line that consists of a tube of electrically conducting material surrounding a central conductor held in place by insulators that is used to transmit radio signals

Mixer - A frequency mixer, is a nonlinear electrical circuit that creates new frequencies from two signals applied to it. In its most common application, two signals are applied to a mixer, and it produces new signals at the sum and difference of the original frequencies

BPF - Band pass filter

LPF - Low pass filter

HPBW - Half power beam width

FWHM - Full width half maximum

Jansky - The Jansky (Jy) is a unit of spectral flux density or spectral irradiance, commonly used in radio astronomy. It is the equivalent of $10^{-26}\mathrm{W}m^{-2}\mathrm{Hz}^{-1}$.

Spectral Irradiance - radiant flux (power) received by a surface per unit area. The SI unit is $\mathrm{W}m^{-2}$.

Radiation Pattern - When we talk about beams in radio astronomy, we are referring to the radiation pattern of a given antenna or source. This is usually the far-field directional dependence of the strength of radio waves from the antenna or the source.

FITS - Flexible Image Transfer System. An image file format commonly used in Astronomy. The file contains a header, tabulated data and different levels of images. (The package that handles fits files in python can be imported from astropy.io import fits).

LCP/RCP - Left (L) and Right (R) Circular Polarization. Usually generated in the hardware as most astronomical objects only emit linearly polarized light. It is easier to generate Stokes parameters using circular polarizations.

PSS - Point Source Sensitivity, a measure of flux correction for each polarization.

1 Guide to the Laboratory

In this section, we're going to discus equipment you will come across in a Radio Astronomy Laboratory. This will involve both instrumentation such as LNA's, bandpass filters etc as well as measurement equipment such as a Vector Network Analyzer (VNA), portable spectrum analyzers and square law detectors. Following this section will be a few practical experiments to try, that will hopefully show the importance of measurement in the laboratory before implementation.

Instruments

Frequency synthesizer and power meter. This exercise will introduce the Frequency synthesizer - an instrument that generates precise microwave frequencies that are locked in phase to a highly stable internal oscillator, usually an oven controlled 10 MHz Crystal oscillator.

Square law detector is a simple device that provides a DC output voltage proportional to the square of input radio frequency signal voltage, because power is proportional to voltage squared the output voltage is therefore proportional to the input power.

Participants will use a test set-up to verify over what range the square law operates correctly by applying an input signal from a microwave frequency synthesizer and measuring the output voltage with a digital voltmeter. Square law detectors are used in radio astronomy receivers, called radiometers.

2 Introduction

These notes will provide some basic theory to help us understand how radio telescopes work and how to do practical radio astronomy with them. Radio waves are a type of electromagnetic wave. The spectrum of electromagnetic waves goes from Gamma rays at short wavelengths (high frequency) to radio waves at long wavelengths (low frequency) as shown in Figure 1. Radio waves are those electromagnetic waves with a wavelength greater than a centimetre. For example, commercial FM radio operates in the frequency range from 88 to 109 MHz, corresponding to a wavelength of about 3 metres. Cellphones operate at a higher frequency of 900 MHz, i.e. a wavelength of 33 cm. We can refer to radio waves either by their wavelength of their frequency. Since all electromagnetic waves travel at the speed of light, c,

$$c = v\lambda, \tag{1}$$

we can easily convert between frequency and wavelength, $\lambda = c/v$ and $v = c/\lambda$.

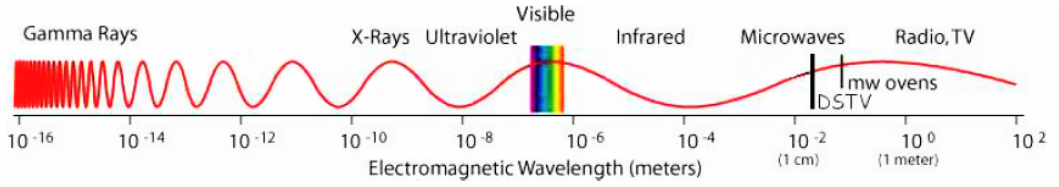

Figure 1: The spectrum of electromagnetic radiation, from high frequency (rays) to low frequency (radiowaves).

Radio telescopes are designed to detect natural radio emission from objects beyond the Earth. The 26m telescope at Hartebeeshoek is a microwave telescope, it operates in the part of the radio spectrum between 30 cm to 1 cm, which means a frequency from 1 GHz up to 30 GHz. Microwave ovens operate at a wavelength of about 13 cm (2.4 GHz) and can be detected by the Hartebeesthoek radio telescope.

Radio astronomy is generally carried out with telescopes that are large compared to the wavelength being observed. This means that they pick up radio waves coming from a small area of the sky, in what is known as the "main beam" of the telescope. For a single telescope, this main beam typically has an angular diameter smaller than a degree, as shown for example in Figure 2.

What do we mean by angular diameter or angular size? Lets think about the size of the full Moon in the sky. The Moon has a physical diameter of 3500 kilometres, yet we see the moon as being about a 0.5 degrees in the sky. Similarly, the Sun has a diameter of 1.4 million kilometres, yet it appears to have the same angular size as the Moon, This is because while about 400 times larger than the Moon, it is also about 400 times further away.

The beam size of the telescope depends on both the diameter of the aperture and the frequency of observation. The beam size tells us the angular resolution of the telescope. Firstly, the diameter of the telescope tells us its collecting area, a larger aperture means a greater collecting area and a smaller beam size. Where networks of radio telescopes operate together, the diameter of the virtual telescope created can be up to 10 000 km, creating a powerful system capable of resolving very small objects (up

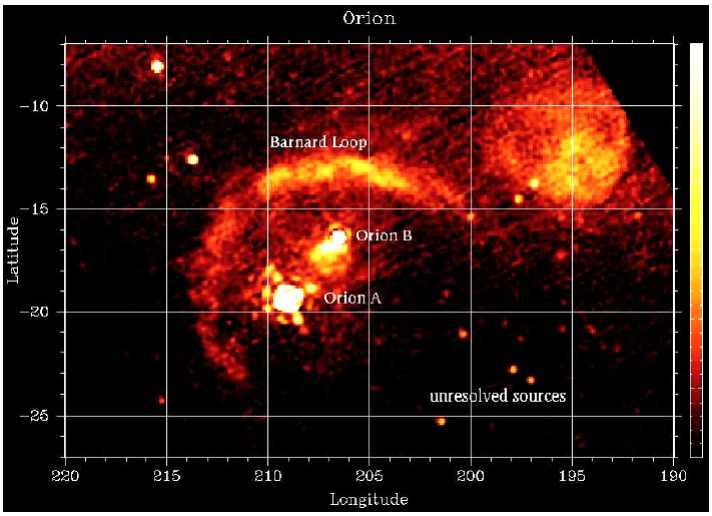

Figure 2: Part of a map of the radio sky made with the Hartebeesthoek telescope at 2.3 GHz. The angular scale is in degrees. The smallest patch of sky the telescope "sees" at this frequency is about one third of a degree. Objects much bigger than this appear approximately their true size (e.g. the Barnard Loop). However small objects all appear smeared out to about one third of a degree in size. Note the "blobs" forming rings around the strong radio sources Orion A and Orion B. These effects are explained in the text. Map by Jonas et al. 1998.

to a millionth of a degree). Secondly, beam size also depends on the frequency (or wavelength). Longer wavelengths (lower frequencies) mean larger beam sizes, If we wanted to build a telescope operating at 5 GHz so that it has the same angular resolution as a telescope at 30 GHz, the diameter would have to be six times that of the 30 GHz telescope.

Outside of the main beam, the telescope is still weakly sensitive to radiation coming from other directions, in what are known as "sidelobes". Man-made radio signals become a problem if they can be detected in these sidelobes, e.g. microwave ovens, wi-fi, bluetooth. These are specific examples of "Radio Frequency Interference" (RFI).

When we look at the sky, our eyes see light which has a continuous, varying distribution of brightness. In the same way, the radio telescope looks at a sky which has a continuous, varying, distribution of radio emission. There are objects of large angular extent producing radio waves, such as hot gas clouds in the Milky Way, and objects of small angular extent, such as distant galaxies, masers and pulsars. Some of the these radio sources will be of larger angular size than the main beam of the telescope and some will be smaller. What the telescope "sees" is the actual radio brightness distribution in the sky *convolved* with ("smeared out" by) the beam of the telescope. The bigger the beam, the more it smears out.

A "classic" radio telescope comprises a circular parabolic reflector with a small receiving element such as a microwave feed horn at the focus to collect the incoming radio waves and pass them to transistor amplifiers in a receiver. A DSTV satellite dish works in exactly the same way and can be used as a mini-radio telescope. The reflector telescope was first described by Scotsman James Gregory in 1663,

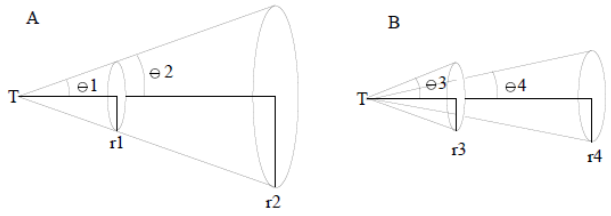

Figure 3: Comparison of physical radius r and angular radius θ. In diagram A, the two objects have different physical radii $r_2 > r_1$, but the same angular radii as seen by telescope T: $\theta_1 = \theta_2$. This applies to the Moon and Sun as seen from Earth. By contrast, in diagram B, $r_4 > r_3$, but $\theta_4 < \theta_3$.

but Englishman Isaac Newton built the first in 1668. American Groote Reber built the first reflector radio telescope, in 1937.

To understand how this system responds to radiation coming from different angles, consider what happens when a plane wave of wavelength, is incident on a circular aperture of diameter D (Figure 4a). Constructive and destructive interference produces a circularly symmetric diffraction pattern, with a central maximum and concentric rings of decreasing strength (Figure 4b). This same pattern describes the response of a circular antenna to plane waves coming from different angles. The first minimum or null occurs at a radius of about $1.2\lambda/D$ radians, so the beamwidth to first nulls is

$$\text{BWFN} \approx 2.4\lambda/D \qquad \text{[radians]}. \tag{2}$$

The beamwidth at the half-power points (HPBW), also called the Full Width at Half Maximum (FWHM) is about half this, as shown in Figures 4c and 4d.

$$\text{HPBW} = \text{FWHM} = 1.2\lambda/D \qquad \text{[radians]}. \tag{3}$$

The angular size of the main beam of the 26-m Hartebeesthoek telescope at four different wavelengths is shown in Figure 5. An "ideal" antenna would produce a beam that would capture 100% of the incoming energy in the centre of the main beam and would have no sidelobes. This antenna would have an "aperture efficiency" ϵ_{ap} of 1. In practice, this is not possible to achieve.

Practically, there two things we can do to make the antenna as efficient as possible. Firstly, we ensure that nothing blocks the radio waves coming into the antenna. We can do this by placing the feed horn off to the side of the reflector, as in a DSTV satellite dish. This is called an "offset paraboloid" design. Secondly, we ensure that the surface is very smooth compared to the wavelength at which the antenna must work. When both these conditions apply, the "best achievable" aperture efficiency is about 0.80. Figures 4c and 4d show an ideal and an actual beam pattern in cross section on linear and logarithmic scales. The "ideal" pattern has been modelled here with a parabolic shape, while the mathematical form of the real pattern is a $\sin x/x^2$ function.

This describes the diffraction pattern where nothing obstructs the path of the waves, providing what is called an "unblocked aperture". The large Green Bank (Byrd) Telescope in the USA (Figure 6a) is shaped like a giant DSTV satellite dish and has an unblocked aperture. Its aperture efficiency is 0.71

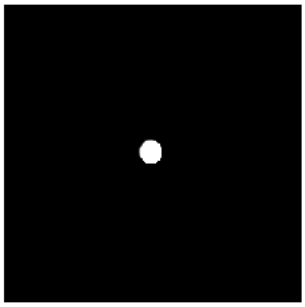

(a) A focusing lens or reflector with a circular aperture.

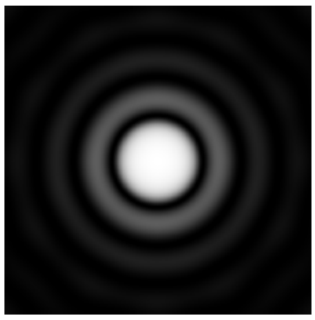

(b) The diffraction pattern (Airy disk) produced by a circular focusing lens or reflector.

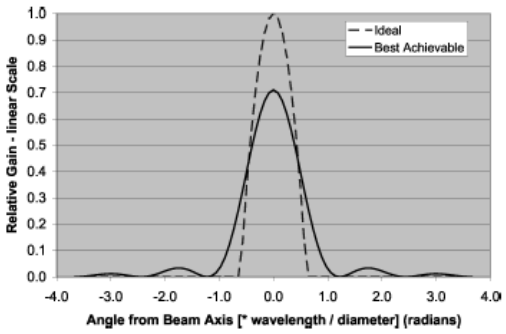

(c) Cross-sections through the beam pattern of an ideal antenna and real antenna, with a linear vertical scale. Note the first nulls at $1.2\lambda/D$

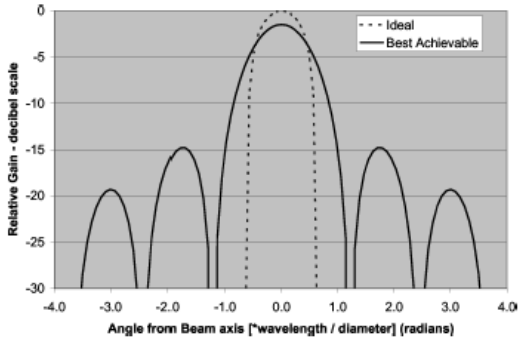

(d) Beam cross-sections of ideal and a typical real antennas, with a logarithmic vertical scale to show the sidelobe structure.

Figure 4: A comparison of point spread functions (PSF, also known as diffraction patterns) of a telescope and their equivalent beam patterns.

at long wavelengths. Often a small reflector of hyperbolic curvature is placed in front of the focus of the main reflector. This is called a "subreflector". The feed horn is then placed at the focus of this second reflector. This is called a Cassegrain optical system and was developed in 1672 by the French sculptor Sieur Guillaume Cassegrain. It is widely used for both optical and radio telescopes, including the Hartebeesthoek 26-m telescope (Figure 6b). The blockage of the aperture by the hyperbolic subreflector, its supports, and the feed housing reduces the maximum achievable aperture efficiency on this telescope to about 0.64.

Often a small reflector of hyperbolic curvature is placed in front of the focus of the main reflector. This is called a "subreflector". The feed horn is then placed at the focus of this second reflector. This is called a Cassegrain optical system and was developed in 1672 by the French sculptor Sieur Guillaume Cassegrain. It is widely used for both optical and radio telescopes, including the Hartebeesthoek 26-m telescope (Fig. 10). The blockage of the aperture by the hyperbolic subreflector, its supports, and the feed housing reduces the maximum achievable aperture efficiency on this telescope to about 0.64.

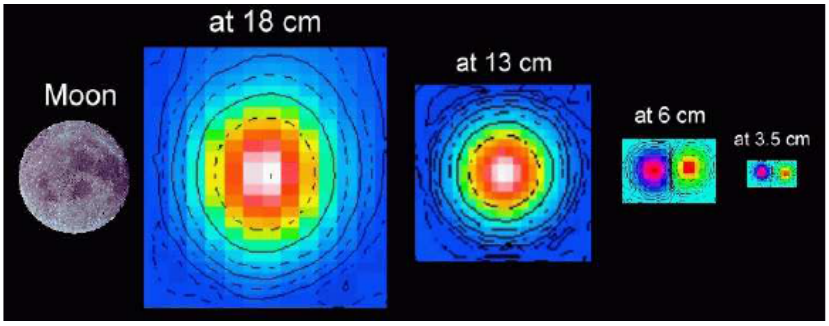

Figure 5: The size of the main beam of the 26-m telescope depends on the operating frequency / wavelength. Here the actual observed main beam at four wavelengths are shown with the angular size of the Moon for comparison. Dual feeds on the 6 and 3.5 cm receivers produce two beams.

If we regard a radio telescope as an electronic circuit, the antenna acts as an amplifier. What is the gain of this amplifier? This depends on the area of sky that it sees. Angular area is called a "solid angle" and the units are radians^2, or steradians (sr). An object with an angular radius θ radians has subtends a solid angle

$$\Omega = 2\pi(1 - \cos\theta) \qquad [\text{sr}]. \tag{4}$$

For small θ,

$$\Omega = \pi\theta^2 \qquad [\text{sr}]. \tag{5}$$

First consider an antenna that is equally sensitive to radiation from all directions. For a telescope that "sees" the whole sky, in polar coordinates we can define this as $\theta = \pi$, this gives a solid angle of 4π sr (or about 41,252 square degrees). Large antennas are primarily sensitive to radiation coming from a small solid angle (7a) and so the gain in the main lobe is much greater than unity.

To explore this in more detail, first we define the total beam solid angle as

$$\Omega_A = \int\int_{4\pi} P_n(\theta,\phi)d\Omega \qquad [\text{sr}] \tag{6}$$

where $P_n(\theta,\phi)$ = beam (power) pattern of the antenna, normalised so that $P_n(0,0) = 1$. One can think of the total beam solid angle as the solid angle that would be subtended by an "ideal" beam with the same gain as at the centre of the actual beam, so that it receives the same amount of power as the actual antenna does integrated over all angles (7b). If we only integrate to the first minimum of the beam pattern, we obtain the main beam solid angle:

$$\Omega_M = \int\int_{mainlobe} P_n(\theta,\phi)d\Omega \qquad [\text{sr}] \tag{7}$$

It can be shown (e.g. Kraus 1986) that the beam solid angle Ω_A depends on the ratio of the square of the wavelength λ to the effective collecting area A_e, which is defined as the product of the physical

(a) The 110m × 100m diameter Green Bank Telescope is the largest steerable radio telescope. It has an offset feed and unblocked aperture, giving an aperture efficiency of 0.71 at longer wavelengths.

(b) The 26-m Hartebeesthoek antenna, showing the aperture blockage from the subreflector and its supports that reduces the aperture efficency compared to the GBT. This has a maximum possible aperture efficiency of 0.64.

Figure 6: The Greenbank and Hartebeesthoek telescopes.

area A_p and the aperture efficiency ϵ_{ap}:

$$\Omega_A = \frac{\lambda^2}{A_e} = \frac{\lambda^2}{A_p \epsilon_{ap}} \qquad [\text{sr}] \tag{8}$$

An isotropic receiving antenna is an antenna that receives equally from all directions, i.e. from a solid angle of 4π steradians, and has a gain of unity. The antenna gain G is the ratio of the solid angles from which an isotropic radiator and the actual antenna receive:

$$G = \frac{4\pi}{\Omega_A} = \frac{4\pi A_p \epsilon_{ap}}{\lambda^2}. \tag{9}$$

The gain of a typical telescope can be anywhere from 10^5 to 10^7, which is the equivalent of 50 dB to 70 dB. Similar to the gain of an amplifier, we write telescope gain in engineering units of decibels:

$$\text{dB} = 10 \log_{10}[G]. \tag{10}$$

Question

If the aperture efficiency of the Hartebeesthoek 26m telescope is approximately 0.5, what is its gain at 1.6 GHz and at 12.5 GHz?

We first need to comment on the polarization of the incoming signals. Detectors operating in the visible

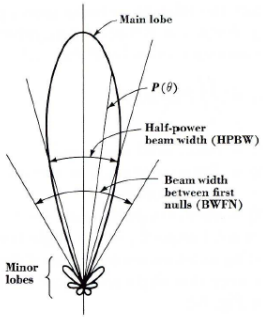

(a) Beam in polar coordinates (Kraus 1986).

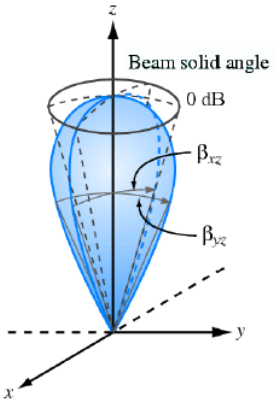

(b) Beam Solid Angle

Figure 7: Polar coordinates and solid angle.

part of the spectrum, such as photographic film or the CCD in a digital camera, capture incoming photons regardless of their polarization state. By contrast, at radio wavelengths the receivers are sensitive to the polarization state of the incoming radiation. It is common practice in radio astronomy to have two receivers attached to each receiving feedhorn, with a splitter feeding left-circularly polarized radiation to one receiver and right-circularly polarized radiation to the other. The total intensity is the sum of what is received in each polarization. In the earlier days of radio astronomy often only one receiver was installed, and the textbooks may assume this in their derivation of equations, although it is normally stated explicitly at some point. This is what gives rise to the factor $\frac{1}{2}$ in Equation 11 below.

We can now define the power w received per unit bandwidth, in each polarization, from an element of solid angle of the sky:

$$w = \frac{1}{2} A_e \int\int_{\Omega} B(\theta, \phi) P_n(\theta, \phi) d\Omega \qquad [\text{W Hz}^{-1}\text{per polarization}] \tag{11}$$

where A_e is the effective aperture (or collecting area) of the antenna [m^{-2}]; $B(\theta, \phi)$ is the brightness distribution of radio emissions across the sky [W m^{-2} Hz $^{-1}$ sr $^{-1}$]; $P_n(\theta, \phi)$ is the normalised power (beam) pattern of the telescope and $d\Omega = \sin\theta d\theta d\phi$ element of solid angle [sr].

What we normally measure in radio astronomy is the integral of the brightness over a radio source. This is called the flux density S of the source:

$$S = \int\int_{source} B(\theta, \phi) d\Omega \tag{12}$$

When the source is observed with an antenna with the power pattern $P_n(\theta, \phi)$ the observed flux density

is given by the integral of the brightness distribution multiplied by the antenna beam pattern:

$$S_o = \int\int_{source} B(\theta,\phi)P_n(\theta,\phi)d\Omega \tag{13}$$

For sources small compared to the beam and in the centre of the beam, $P_n(\theta,\phi) \approx 1$. For extended sources with simple geometries, simple analytic functions enable S_o to be corrected, and these will be discussed later. A simulation of how the finite width of the telescope beam "blurs" the true radio brightness distribution is shown in Figure 8. The SI unit of flux density would be W m^{-2} Hz^{-1}. However, the radio emission is very weak as the radio emitters are very far away, and the unit known as the Jansky [Jy], after the radio astronomy pioneer Karl Jansky, was adopted in 1973. It is defined as 10^{-26} W m^{-2} Hz^{-1}.

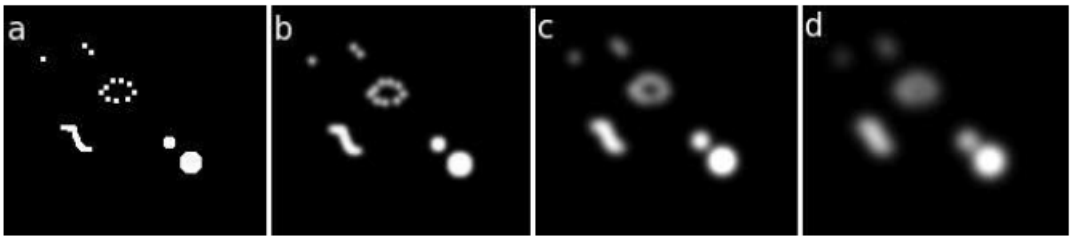

Figure 8: (a) Simulated true radio source brightness distribution, convolved with beams of width (b) 5 units (c) 10 units (d) 15 units.

Radio astronomy appears as something of a blend of astronomy and basic electric circuit theory. This derives from the fact that the radio telescope can be considered as an electric circuit, and the object being observed can be considered as a resistor at a particular temperature connected to the first amplifier in the receiver (by radio waves rather than by wires). For some astronomical objects the temperature that we measure is meaningful as a physical temperature. For others it is not, depending on the radiation mechanism involved, and we therefore refer to the "brightness temperature" T_B for these emitters. Astronomical masers provide an example of this. The gas producing the emission may have a physical temperature of less than 200K, but the very intense stimulated emission of the maser could have a brightness temperature of 10^{12}K.

For a blackbody radiator, the brightness B is given by

$$B = \frac{2h\nu^3}{c^2}\frac{1}{\exp[h\nu/kT]-1} \qquad [Wm]^{-2}\mathrm{Hz}^{-1}\mathrm{sr}^{-1}, \tag{14}$$

where h is the Planck constant (6.63×10^{-34} [J s]; ν is the frequency [Hz]; c is the velocity of light (3×10^8 [ms^{-1}]); k is the Boltzmann constant (1.38×10^{-23} [J K^{-1}] and T is the temperature [K].

From Fig. 14 we can see that for all objects with temperatures more than a couple of degrees above absolute zero, the brightness peak occurs well above the operating range of radio telescopes. Hence we are working in the range where $h\nu << kT$, so the Rayleigh-Jeans law applies and the brightness

is proportional to the temperature:

$$B = \frac{2kT}{\lambda^2} \qquad [\text{W m}^{-2}\text{Hz}^{-1}\text{sr}^{-1}]. \tag{15}$$

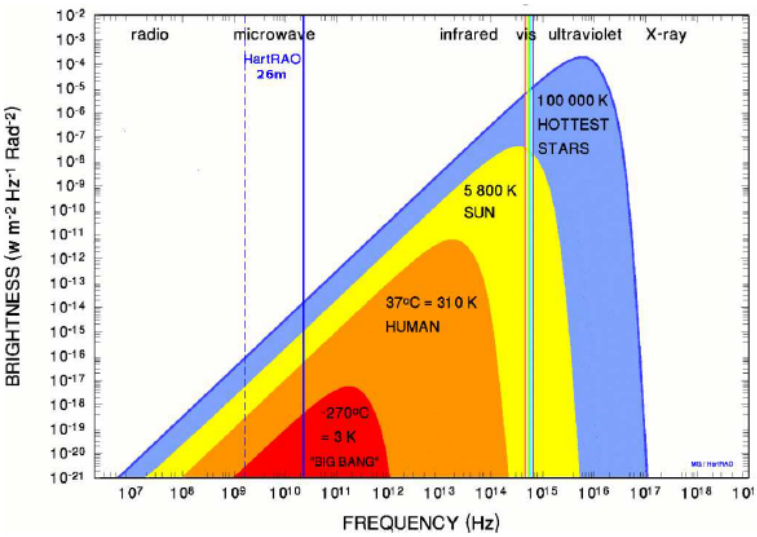

Figure 9: Blackbody radiation from solid objects of the same angular size, at different temperatures

If we observe the radiation from a discrete source which has an effective temperature T and subtends a solid angle Ω_s, the source flux density (in SI units) is simply the product of the brightness and the source solid angle:

$$S = \frac{2kT\Omega_s}{\lambda^2} \qquad [\text{W m}^{-2}\text{Hz}^{-1}]. \tag{16}$$

Question

If we take the brightness temperature of the Sun at a wavelength of 10cm to be 10 000 K, what is the flux density in SI units and in Jy? (Remember 1 Jy = 10^{-26} [W m^{-2}Hz^{-1}])

Question

The nearest naked eye star is α Centauri. This is a binary system of two Sun-like stars. What is its flux density at $\lambda = 10$cm?

More generally, if the temperature distribution over the emitter is not uniform, the flux density becomes

the integral of the temperature distribution over the object:

$$S = \frac{2k}{\lambda^2} \int \int_{source} T(\theta, \phi) d\Omega \qquad [\text{W m}^{-2}\text{Hz}^{-1}]. \tag{17}$$

For a solid object such as a planet like the Earth, the optical depth through the object is very large, and the observed temperature $T_b \approx T_e$, the actual temperature. For objects such as gas clouds, T_b will depend on the optical depth τ_c, the physical temperature being denoted by the electron temperature T_e:

$$T_b = T_e(1 - e^{-\tau_c} \qquad [K] \tag{18}$$

For small optical depths the brightness temperature approximates to:

$$T_b = T_e \tau_c \qquad [K] \tag{19}$$

We can regard the observed radio source as being equivalent to a resistive load on the input to the first amplifier in the receiver system on the telescope. The power w per unit bandwidth received at the terminals of a resistor of temperature T would be:

$$w = kT \qquad [\text{W Hz}^{-1}]. \tag{20}$$

The radio source is not connected to the amplifier by wires, as a resistor would be. It is connected by the radio waves emitted by the source and received by the antenna. This lets us consider it as a resistor and we can equate the power received from the source with power received from a resistor with the same temperature. We call this temperature the measured "antenna temperature" T_A of the radio source. It has nothing to do with the physical temperature of the antenna.

The total energy received per unit bandwidth in the two polarizations is then the effective collecting area times the observed flux density S_o, which we equate to the power received from the equivalent resistor:

$$w_{lcp+rcp} = A_e \int_{Omega} \int B(\theta, \phi) P_n(\theta, \phi) d\Omega = A_e S_o = k(T_{Alcp} + T_{Arcp})[\text{W Hz}^{-1}]. \tag{21}$$

To obtain the true flux density S we introduce a size correction factor K_s. For sources that are very small compared to the beam size, $K_s = 1$, and $S_o = S$, but the correction must be taken into account if the source size is a significant fraction of the beam size. Details of the size correction are given later. Simplifying Equation 21, we obtain the true flux density of the source by summing the antenna temperatures measured in left- and right-handed circular polarization and allowing if necessary for finite source size through K_s:

$$S = \frac{k(T_{Alcp} + T_{Arcp})K_s}{A_e} \times 10^{26}[\text{Jy}]. \tag{22}$$

It is important to note that the flux density of a radio source is intrinsic to it, and the same flux density should be measured by any properly calibrated telescope. However the antenna temperatures measured for the same emitter by different telescopes will be proportional to their effective collecting

areas. We can only calculate the source flux density if we know the effective aperture (collecting area) at the frequency being used, so we rewrite Equation 22 and substitute the constants, to give:

$$A_e = \frac{1380(T_{Alcp} + T_{Arcp})K_s}{S_o}[\mathrm{m}^2] \tag{23}$$

This lets us calibrate the radio telescope at each frequency of interest. We carry out scans of standard calibrator sources (Ott et al. 1994) and measure the peak antenna temperature in each polarization. The calibrator flux densities are obtained from the formulae given by Ott et al. Substitution into the above equation provides the effective aperture (collecting area). The physical collecting area Ap is obtainable from the known diameter of the telescope (25.9 m for the Hartebeesthoek telescope). The aperture efficiency ϵ_{ap} can then be obtained at each frequency:

$$\epsilon_{ap} = \frac{A_e}{A_p} \tag{24}$$

For convenience, we often refer to the Point Source Sensitivity (PSS), which is (correctly) the number of Kelvins of antenna temperature per polarization obtained per Jansky of source flux density. This is also known as the 'DPFU' or 'Degrees per Flux Unit', the flux unit being the old term for the Jansky. For small antennas (such as the Hart 26m) the PSS is often used in the inverse way, i.e. the number of Janskys of flux density required to produce one Kelvin of antenna temperature in each polarization. For the Hartebeesthoek telescope, the PSS, expressed in the latter form, is typically about 5 Jy/K per polarization. The PSS in each polarization is simple to determine experimentally, from the antenna temperatures measured for calibrator sources of known flux density (remembering that for an unpolarized source, half the total flux density is received in each polarization):

$$\mathrm{PSS}_{lcp} = \frac{(S/2)}{K_s T_{Alcp}} \quad \text{and} \quad \mathrm{PSS}_{rcp} = \frac{(S/2)}{K_s T_{Arcp}} \quad [\mathrm{Jy\ K^{-1}per\ polarization}] \tag{25}$$

Theoretically the values for the two polarisations should be the same; in practise there is always a small difference between them, and data from each polarization should be corrected using the value appropriate to that polarization.

If the angular size of emitting object is known and is small compared to the beam size, the emitter's brightness temperature T_b can be estimated from the ratio of the beam solid angle Ω_A to the source solid angle Ω_s:

$$T_b = \frac{\Omega_A}{\Omega_s} T_A \quad [\mathrm{K}]. \tag{26}$$

The Hartebeesthoek 26-m radio telescope is currently equipped with receivers to cover selected bands used for radio astronomy: 18cm / 1.6GHz, 13cm / 2.3GHz, 6cm / 5GHz, 5cm / 6.0GHz, 3.5cm / 8.5GHz, 2.5cm/ 12GHz, 1.3cm / 22GHz. In general, we want each receiver to cover as wide a band as possible. However, some receivers are designed only to observe emission at one particular frequency from a specific atom or molecule, and these have a relatively narrow bandwidth. For comparison, the bandwidth of the receiver in an FM radio is 20MHz, as it covers 88 to 108MHz. When built by NASA in 1961 to track spacecraft, the 26-m antenna had one receiver, operating at 30cm / 960MHz.

3 Receivers

The purpose of a radio antenna is to generate small alternating currents from incoming radio waves, it can have different shapes to optimise it for the frequency it operates at and its purpose. The receiver then takes those incoming currents and processes them using electronics and signal processing techniques. Generally when we refer to the receiver of a telescope, we are referring to the element that converts incoming radio waves to a current (feed horn or a feed point in a dipole antenna), all of the analogue electronics and any digital processing that takes place. Figure 11 shows a Cassegrain radio antenna with a parabolic primary reflector and an additional secondary reflector, the "front end" of the receiver consists of the feed horn and the low noise amplifiers (LNA's) immediately after the feed. The "back-end" of the receiver is all electronics after the LNA's including any digital signal processing (DSP) that happens in the computer.

A more detailed version of a typical conventional microwave receiver is shown in Figure 12. The incoming signals are very faint and noise-like. If the output of a receiver is connected to a loudspeaker, the signal sounds like a hiss, the same hiss one hears if a radio is tuned off-station. The internal noise in the amplifiers is generally much larger than the signal. To maximise sensitivity we need to minimise the noise of the amplifiers. This is generally done with specially designed amplifiers that can be cooled in refrigerators, in our case to 16 K, or $-257°$C.

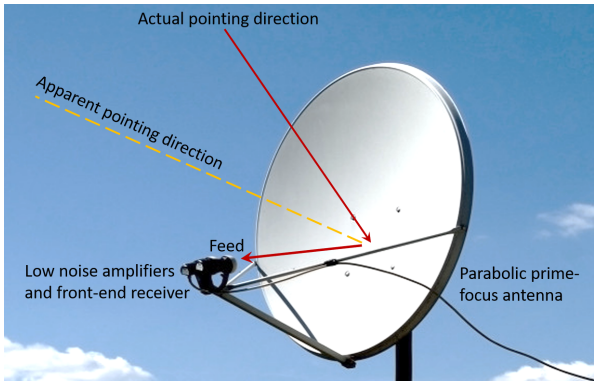

Figure 10: A parabolic prime-focus reflector satellite antenna. The dish is off-axis to avoid the feed blocking the aperture.

Over a limited band, the noise-like signal from the sky and the noise from the amplifiers in the receiver can be treated as though they were produced in resistors with specific absolute temperatures. The effective noise temperature of a receiver T_R depends on the noise temperature Tn and gain G_n of each amplifier:

$$T_R = T_1 + \frac{T_2}{G_1} + \frac{T_3}{G_1 G_2} \qquad \text{[K]}. \tag{27}$$

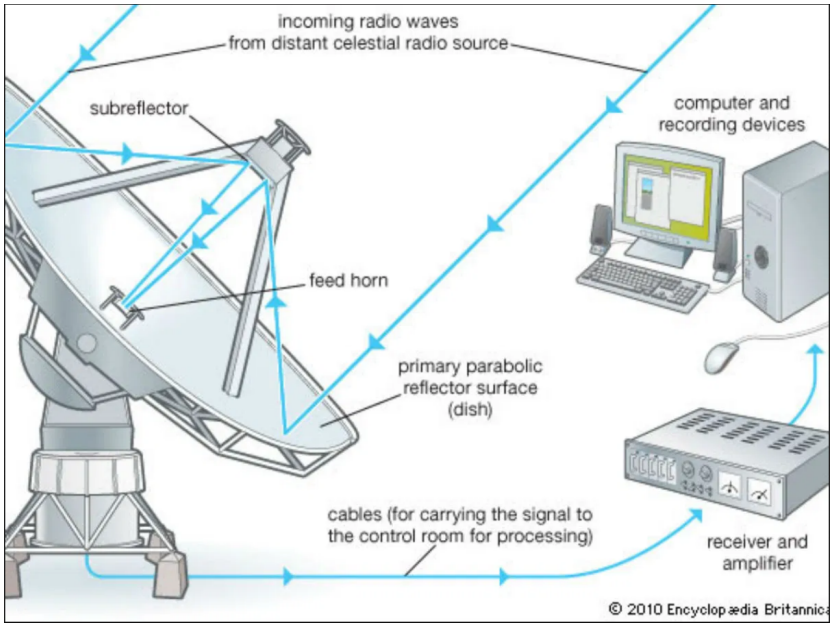

Figure 11: Diagram of a radio telescope. At the feed horn we position low-noise amplifiers, this part of the receiver is known as the "front-end" receiver. After the "low-noise amplifier" (LNA), the signal is then processed with filters, RF amplifiers and is usually broken down into smaller chunks of bandwidth by a mixer to generate an "intermediate frequency" (IF). This can be further amplified and sent to a computer for "digital signal processing" (DSP). We refer to all electronics and processing after the LNA to be the "back-end".

Question

In the example shown in Figure 12, what are the contributions to the receiver temperature from the first three stages? Which amplifier is most critical in keeping T_R small?

The receiver noise temperature T is often quoted in the form of a "noise figure" F, relative to a nominal ambient temperature of 290 K (17°C):

$$F = 1 + T/290 \tag{28}$$

and can also be expressed in decibels:

$$F_{\rm dB} = 10 \log_{10}(F) \qquad [\rm dB] \tag{29}$$

Question

What is the noise temperature in dB of the receiver in Figure 12

Signal losses in waveguide and co-axial cable are large at microwave frequencies, so mixers are used to convert signals down to a lower frequency that can be passed through many metres of cable to the control room where the signal detecting instruments are located. The attenuation in passive components both reduces (attenuates) the signal strength and introduces extra noise. Defining the signal loss L ($\inf > L > 1$) of the component as the reciprocal of the gain G ($0 < G < 1$), the noise temperature T_L of a lossy component at a physical temperature T_{LP} will be

$$T_L = (L-1)T_{LP} \qquad \text{[K]} \tag{30}$$

Question

In a section of waveguide at ambient temperature, 85% of the signal is transmitted so $G = 0.85$. What noise temperature is introduced by waveguide?

If this wavegeuide is used to connect the feed horn to the first amplifier, the noise temperature T_{RT} of the waveguide plus receiver will become

$$T_{RT} = T_L + LT_R = (L-1)T_{LP} + LT_R \qquad \text{[K]} \tag{31}$$

In the example given in Figure 12, what would the receiver temperature be with the added section of waveguide.

The power w at the output of the mixer in Figure 12 is given by:

$$w = G_1.G_2.G_3.k(T_A + T_1)\Delta\nu + G_2.G_3kT_2\Delta\nu + G_3kT_3\Delta\nu \qquad \text{[W]} \tag{32}$$

where T_A is apparent temperature of the sky as seen by the antenna [K]; k is the Boltzmann's constant and $\Delta\nu$ is the bandwidth [Hz].

The radiometer is the basic instrument for measuring the power of the incoming signal. Radiometry is analogous to photometry in optical astronomy. The simplest form of radiometer is the "total power" type shown in Figure 12. The signal measured by the radiometer will vary if the gain changes in any of the amplifiers (or the loss changes in any of the passive components such as waveguide or cables), and this could be mis-interpreted as a change in the signal from the sky. However changes in gain can be measured if a noise signal of constant strength is injected at regular intervals immediately after the feed horn, before the first amplifier. This signal is detected by the software reading the output of the radiometer, which then adjusts the output to keep the measured strength of the injected signal constant. This technique is is known as "noise-adding, gain-stabilised" radiometry, and is available on the Hartebeesthoek 26-m telescope. The varying water vapour content in the atmosphere acts as a variable attenuator for the incoming signal from space, and adds its own noise to the signal. If two feeds are installed next to each other on the telescope, the effects of the atmosphere will be largely common to both of them, but they will be looking at different points in space. If we are measuring signals from radio sources whose angular sizes are smaller than the separation of the beams from the two feeds, we can switch rapidly between the two feeds and just detect the difference in signal. This technique is called "Dicke-switched" radiometry, after its inventor. On the Hartebeesthoek 26-m telescope, the 6-cm and 3.5-cm receivers are equipped with dual feedhorns and can operate in this mode. The old

receiver mounted on the east wall in the Visitors Centre is the original dual-feed system for 6 cm wavelength.

When the telescope looks at a radio source in the sky, the receiver output is a combination of energy received from several different sources:

- Behind the radio source whose flux density we want to measure is the cosmic microwave background (CMB) coming from every direction in space. This is the relic radiation left as the first atoms formed 380 000 years after the Big Bang. The Black Body temperature of the CMB T_{cmb} has now decreased to 2.7 Kelvins, thanks to the expansion of the Universe. This produces a brightness temperature T_{bcmb}, which depends on frequency.
- The emission from the radio source to be measured, which produces a source antenna temperature T_A.
- Radiation from the dry atmosphere T_{at}. Optical depth, τ (Equation 18 depends on elevation angle.
- Radiation from water vapour in atmosphere T_{wv} (τ depends on weather); important above 10GHz. Optical depth depends on elevation angle.
- Radiation from the ground in the beam sidelobes T_g, depends on elevation angle.
- The amplifiers in the receivers generate their own electronic noise and so produce a receiver noise temperature T_R.

The sum of these parts is called the "system temperature" T_{sys}. All the components are frequency-dependent. Summing from the most distant noise contributor to the nearest we have:

$$T_{sys} = T_{bcmb} + T_A + T_{at} + T_{wv} + T_R \qquad \text{[K]} \tag{33}$$

The most basic measurement that can be made of a radio source is its signal strength over a defined band, by radiometry. This is like what our eyes do when we look at light sources of different brightness, such as the Sun, a light bulb, a candle or a star. The output signal from the radiometer is proportional to T_{sys}, which is what we want to measure, and from which we then want to extract T_A, the signal from the source of interest. We will describe one way of extracting T_A from T_{sys} in the next section. However, because the input signal is noise-like, the output signal shows fluctuations. The output voltage in each polarization will show fluctuations with a root mean squared size, T_{rms}. The size of the fluctuations is directly proportional to T_{sys}, but also depends on the square root of the receiver bandwidth $\Delta\nu$, and the length of time for which the signal is averaged, which we call the "integration time", t:

$$\Delta T_{rms} = \frac{T_{sys}}{\sqrt{\Delta\nu t}} \qquad \text{[K]} \tag{34}$$

This is called the "radiometer sensitivity equation". The bigger the bandwidth and the integration time, the smaller the noisey fluctuations will be in the output signal. We can generalise this to allow

for losses associated with specific types of receiver, which will increase the fluctuations, and for the averaging of n repeated scans, which will reduce the fluctuations:

$$\Delta T_{rms} = \frac{K_R T_{sys}}{\sqrt{\Delta\nu t n}} \qquad [\mathrm{K}] \tag{35}$$

where K_R is the sensitivity constant of the instrument. Its value is 1 for a simple radiometer.

The smallest change in antenna temperature ΔT_{min} that can realistically be detected is normally taken as three times the rms noise:

$$\Delta T_{min} = 3\Delta T_{rms} \qquad [\mathrm{K}] \tag{36}$$

In the same way, we can usefully define the minimum detectable flux density S_{min}, by making use of Equations 22, 35 and 36:

$$\Delta S_{min} = \frac{3K_R k T_{sys}}{A_e\sqrt{\Delta\nu t n}} \times 10^{26} \qquad [\mathrm{Jy}] \tag{37}$$

These equations let us check that the measured noise in the data matches that expected, i.e. that the receivers are functioning correctly, and it lets us predict whether radio sources of a given flux density should be observable within a given integration time.

Now we need to put all this theory together to make actual measurements of radio sources in space. The simplest way to measure the intensity of a compact radio source in the sky, i.e. one that has an angular size much smaller than the telescope beam, is to park the telescope a little west of the current position of the radio source in the sky, and use the rotation of the Earth to let the telescope beam drift steadily across the source. Not surprisingly, this observing method is called a drift scan. The output of the radiometers will be the convolution of the antenna beam pattern (e.g. see Figure 13a) with the brightness distribution of the source (e.g. Figure 8). Looking back at Equation 33, we can see that this method has the advantage that T_{cmb}, T_{at}, T_g and T_R should all be constant, and only TA should change, this being what we want to measure. If the radio source has an angular size much smaller than the angular size of the beam, the output from the radiometer during the scan is effectively an east-west cross-section of the beam of the telescope. An example is shown in Figure 13b. The passage of the main beam across the radio source is obvious in the centre, and the first sidelobes are weakly seen on each side. The noise described by equation 33 is clearly visible. Looking at the minima across the scan, we can see a slow drift in the signal level. This could be due to changing atmospheric conditions, or to a slow change in gain of the receiver system. To measure the signal strength we need to establish the slope between the first nulls by drawing a line between them. Then we measure the height above that line at the centre of the beam. This gives us the antenna temperature TA of the source. From a drift scan such Figure 13b, we can also measure the full width at half maximum (FWHM). This is commonly used as a descriptor for the width of the telescope beam, together with the "beamwidth to first nulls" (BWFN), and we can compare this to what was earlier calculated theoretically. Note that scans in Right Ascension are broadened by the secant of the Declination of the source. The true FWHM or BWFN is the value measured from a drift scan, multiplied by the cosine of the Declination of the source at the epoch of observation.

Question

If we compare Figure 13a with Figure 4b, why are the sidelobe rings broken up into a symmetric pattern of "blobs"?

Compare the sidelobes in Figure 13b with those of Figure 4c The first sidelobes can be seen on either side of the main beam - compare with Fig. 6.

If this is a calibrator source, then the point source sensitivity in this polarization is immediately obtained from the flux density S at the observing frequency (Ott et al. 1994), using Equation 25. Once this has been determined, the flux density of unknown sources can be found from their observed antenna temperatures. For an unresolved radio source, the full width at half maximum (FWHM) of the scan equals the half-power beamwidth. If the source is somewhat extended, the width will be broadened, as discussed previously.

Types of Radiometer

A radiometer is a way of measuring the total power of a signal. In radio astronomy, we are interested in signals that are weak compared to noise and in our receiver are very noisy components, such as the low noise amplifiers. Therefore we need a way of calibrating the gain in our receiver, and tracking it over time to make sure that we can separate out our signal from the noise. When talk about the different types of radiometer, we are talking about the different types of methods of gain calibration.

The most standard radiometer is a total power radiometer.

The total power radiometer equation is:

$$\sigma_T = T_{sys}\left[\frac{1}{\Delta\nu\tau} + \left(\frac{\Delta G}{G}\right)^2\right]^{\frac{1}{2}} \tag{38}$$

The noise term σ_T is given by the noise variance which depends on the RF bandwidth ($\Delta\nu$), and the integration time τ. The gain fluctuation given by ΔG, produces a signal that cannot be distinguished from the noise temperature of an astronomical sources. As a result, the variance is given by the ratio of the gain fluctuation over the overall gain of the receiver, G.

The total power radiometer can detect power variations, and is sufficient for applications where the received signal is bright. However this is not suitable for radio astronomy, as we have no way of distinguishing our source from the background noise.

The earliest type of receiver that measures the gain of the receiver itself, is a **Dicke Switch Radiometer**. This rapidly switches between a calibration load and the sky signal to characterize the gain as a function of time. The Dicke Switch uses something called a lock in amplifier which can extract a waveform from a noise environment. When both the load (T_{ref}) and the signal are equal, the lock-in-amplifier returns a zero measurement and hence a measurement of the gain alone can be measured. We can

write the resulting temperature change from the gain fluctuation as:

$$\Delta T = \frac{\Delta G}{G}(T_S - T_{ref}) \tag{39}$$

The disadvantage of this type of gain calibration technique, is that the duty cycle of the square wave which controls the lock0in-amplifier, is only 50%. That means that 50% of the time, the radiometer is not observing. This means we have a reduction in sensitivity of $\sqrt{2}$ since our antenna is only measuring half of the time. The limit of obtainable sensitivity is hence given by the radiometer equation as:

$$\sigma_T = 2 \times T_{sys}\left[\frac{1}{\Delta\nu\tau} + \left(\frac{\Delta G}{G}\right)^2\right]^{\frac{1}{2}} \tag{40}$$

This factor of two of performance degradation is usually a good trade off for improved stability.

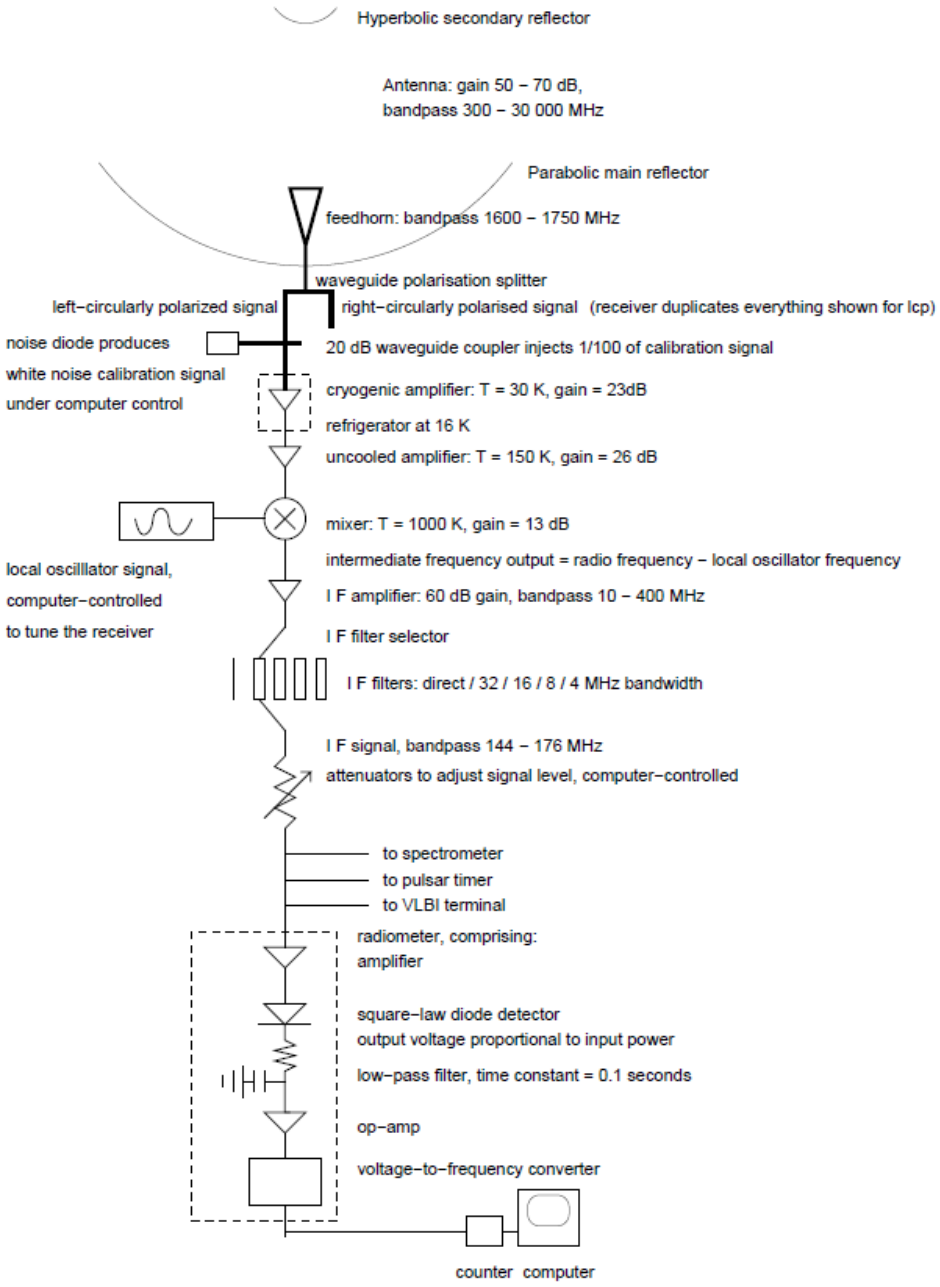

Figure 12: Main components of a typical microwave receiver and radiometer.

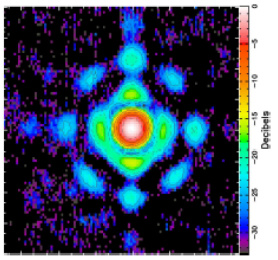

(a) Actual beam pattern at 2300 MHz of the Hartebeesthoek telescope. Contour levels are at 3dB intervals, so that each contour is half the level of the previous one.

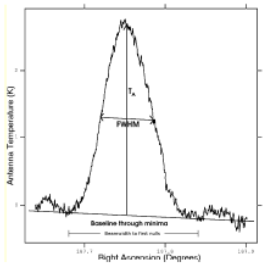

(b) Typical drift scan through an unresolved radio source. The signal is equivalent to a horizontal cross-section through the centre of the antenna beam pattern.

Figure 13: Real beams from Hartebeesthoek.

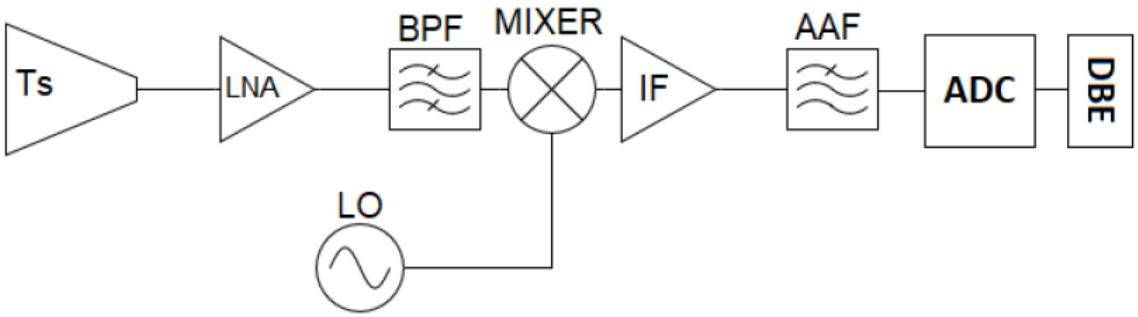

Figure 14: Total Power Radiometer

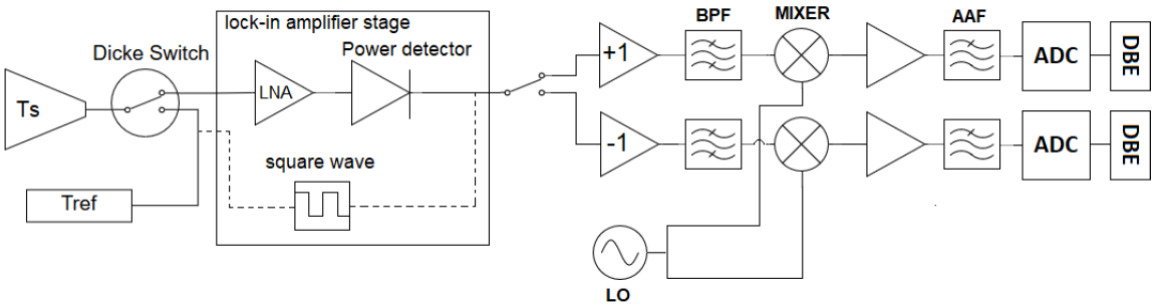

Figure 15: Dicke Switch Radiometer

4 Interferometry

Interferometry is a technique used in radio astronomy that superimposes electromagnetic waves creating interference to extract information. Interferometry allows us to get a much higher resolution than with a single dish telescope. With a single dish, we are limited to the diffraction pattern of the telescope. The criterion for a telescope's resolving power is such that the central maximum of an Airy disk (from a star) should like on the first minimum of the other.

$$\theta_{\text{rad}} = 1.22\lambda/D \tag{41}$$

For longer wavelengths, we need a much bigger diameter dish to get the same resolution as we would see at higher wavelength images (visible light, UV etc).

We can consider two telescopes separated by a large distance L, looking at an object, O. The light from this source see will travel different path lengths to arrive at each telescope, it will also take a different amount of time to arrive at telescope 1 than telescope 2. We refer to this difference in arrival time as a path delay. In Figure 16 we can see the path length P' has been derived by considering the distance between two antennas to be some integer number, n of observing wavelengths, $L = n\lambda$.

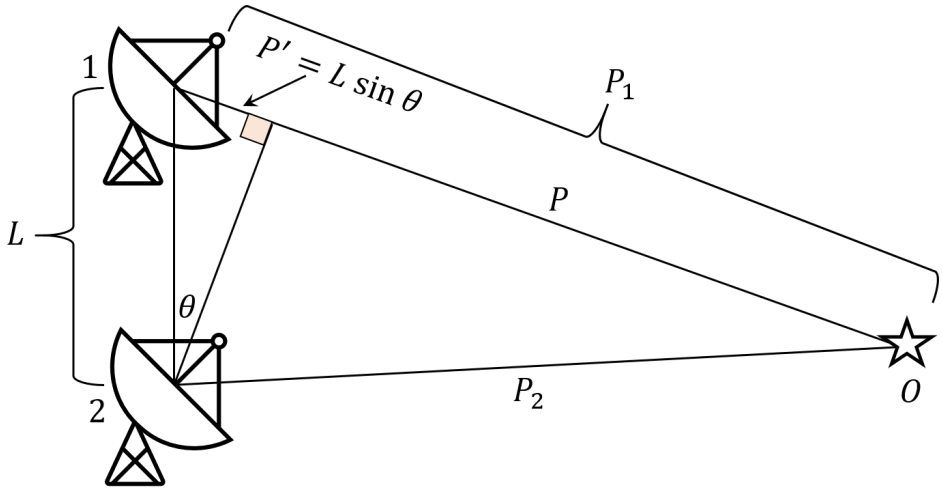

Figure 16: A diagram showing the geometry of an interferometer. The interference pattern arises from the path length difference at the two antennas from the source, O.

We can see that the waves from this source will travel along different path lengths, P_1 and P_2, where $P_1 > P_2$ and P' is the extra amount the wave has had to travel such that $P_1 = P + P'$. We can see that $P' = L\sin\theta$. For constructive interference, P' must be an integer number of wavelengths such that:

$$L\sin\theta = m\lambda. \tag{42}$$

As the Earth turns, θ varies. The fringes are evenly spaced by the angle for which $m = 1$:

$$\sin\theta_f = \lambda/L = \lambda/n\lambda = 1/n \tag{43}$$

since θ_f will be small, $\sin\theta_f \approx \theta_f$ (in radians) and

$$\theta_f = 1/n \qquad \text{rad}, \tag{44}$$

where n is the number of wavelengths λ in the baseline L.

Radio vs. Optical

For a 21 km baseline ($L = 21$km) at a wavelength of 21 cm (~ 1.43 GHz), we get a resolution of $\approx 10^{-5}$ rad or 2". This is a similar resolution to that of an optical telescope.

Correlation

In practice, we don't know the path lengths, so we need to estimate this from differences in arrival times. We now need to consider how to get an image from delay times. The process of making an image from two or more voltage signals from the same number of telescopes is done in a process called correlation.

Forget about pixels!

We can think of a radio telescope as being a radio-wave bucket with a detector (or receiver) at its focus. The receiver takes the incoming radio waves and converts them into a time-varying voltage. We need to start thinking about making images using time delays.

Correlation is an important function of the radio receiver. The first consideration we must make is that the receivers are operating at exactly the same frequency. We do this by transmitting the signal at each radio telescope to check they are at the same frequency. To ensure that the frequency of the receiver is fixed, we must apply a phase lock system. In a super-heterodyne receiver, we must down convert the signal to IF band. A phase lock loop compares the LO used in down-conversion to an external reference frequency, and sends an error signal back to the LO to keep it in perfect phase lock with the reference signal. Each antenna receives the external reference signal from the same source, so all receivers are locked to the same frequency. Any error in the phase results in an error signal that is fed back to the oscillator to adjust it's frequency to maintain exact frequency tuning.

Most interferometers make use of optical fiber multiplexing which takes multiple signals through a single optical fiber to a central control room where the signals are correlated. The IF (down converted signal) from each receiver is noise like. If both signals look the same, how do we tell them apart? A source signal will be correlated between two antennas, while locally generated noise signals will not.

For time varying voltages V_1 and V_2, the correlation is found by multiplying them, with a delayed signal t_g (not to be confused with the geometric delay, τ_g).

$$r =< V_1(t)V_2(t) > \tag{45}$$

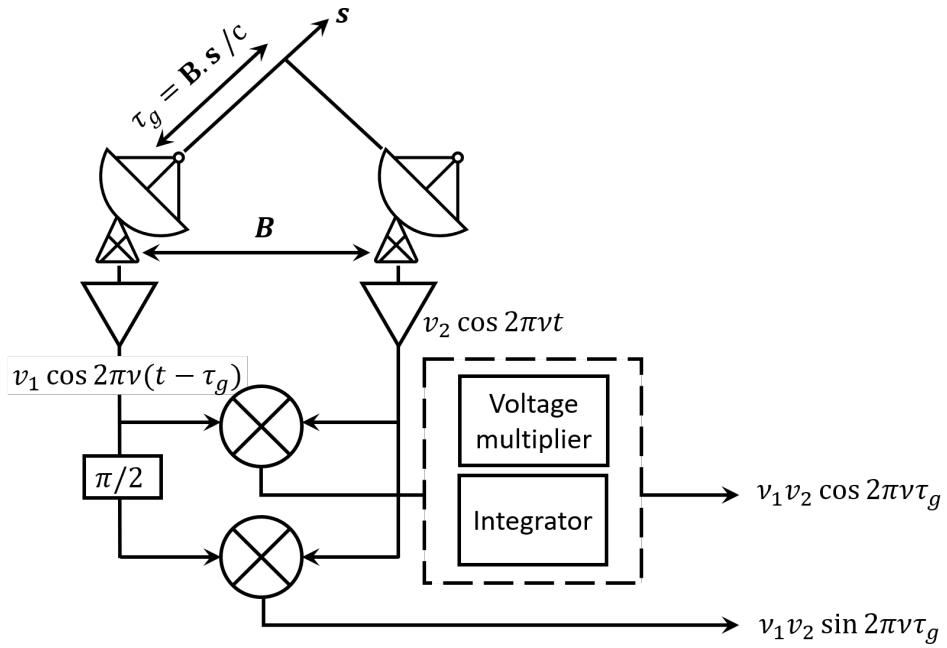

Figure 17: Figure showing values from correlator

where we find the expectation value, found by averaging over an integration time. For a single frequency, time-varying signal:

$$V_1(t) = \nu_1 \cos(2\pi\nu(t - \tau_g)) \tag{46}$$

and

$$V_1(t) = \nu_2 \cos(2\pi\nu t) \tag{47}$$

We can rearrange to get r as

$$r = \nu_1\nu_2 \cos(2\pi\nu\tau_g) \tag{48}$$

Since the geometrical delay τ_g changes due to the Earth's rotation, the relatively slow varying cosine term causes the oscillations that represent the motion of the source through the interferometer fringe pattern. The rate of fringe oscillations is called the **natural fringe rate**. The fringe frequency is:

$$\nu_F = dw/dt = -\Omega_e u \cos\delta \tag{49}$$

where Ω_e is the ration rate, w is the spatial frequency corresponding to the projected baseline z-component given by coordinate transformation !

Demonstration

You are going to see a demonstration with a two-element interferometer. You are going to see a demonstration with a two-element interferometer. It is very simple, it just uses a **mixer** to add the

signals from two dishes, and it does not track, so as the sky rotates objects will move through its field of view. The frequency is 12 GHz, and the bandwidth is narrow enough so that you can treat the radiation as mono-chromatic. We will point it near the sun, since the sun is the brightest radio source in the sky, and it is relatively easy to aim at. As the sun moves across the sky, it will move through the response patterns of the individual antennas and interferometer.

There are two effects here. Firstly, if we look at the output of just one dish: the dish has a diameter 1.2 meters, and so it is sensitive to radiation only from a certain angle on the sky. The response is approximately Gaussian. The detector measures the square of the electric field (so the detector output is always positive) averaged over 0.05 seconds. Since we're working at 12 GHz, one period is 8.33×10^{-11} seconds, so it is averaging over many, many cycles of the underlying waveform. Secondly, if we connect both dishes and look at the interferometer output, we're adding the complex signals from the two antennas and our detector measures the sum of the two signals.

In the mixer, the signals add as vectors, so the two signals could add destructively or constructively, which depends on the time delay between when the signal from the first antenna hits the mixer to the time that the signal from the second one does. This delay will cause second signal to be phase-shifted with respect to the first. If the signals going into the mixer are equal in amplitude and in phase, then the output from the mixer has twice the amplitude of each individual signal. If the signals are exactly out of phase (and equal) then the output of the mixer would be exactly 0.

The first part of that phase shift is just given by the geometry, this is called the geometrical delay. If the line between the two antennas (the baseline) is exactly perpendicular to the direction to the sun then there is no delay difference, and thus no phase shift, and the two signals would add constructively. However, as the sun moves across the sky, the direction to the sun rotates with respect to the baseline, and so there will be some delay.

Note

We need only worry about the difference in delay between the two antennas, of course the radio waves left the surface of the sun ∼8 minutes ago, but all that matters for us is the much smaller differences between the paths to the two antennas. In fact, there is a further phase-shift between two antennas because the cables are not of exactly equal length. However, this phase shift remains constant with time. So as the sun moves, we expect an alternating pattern of maxima and nulls, as the two signals go in and out of phase.
Other information you will need: Dish Diameter: 1.2 meters; Frequency: $\nu = 12 GHz$*; Speed of light:* $c = 3.00 \times 10^8 ms^{-1}$*; Wavelength:* (c/ν)*=0.025 meters ;Distance between dish centres: 5.0 meters.*

Questions

1. If we only look at the signal from only one dish, and we have the dish pointed exactly at the sun at (local solar) noon, what do you expect the output to look like for the period say from 10 minutes before noon to 10 minutes after?
2. Now if we add the second dish to make the interferometer, and point it exactly at the sun at noon, with the baseline oriented exactly East-West. How much time do you expect between the two nulls? (*Hint: think in terms of difference in the geometric delay between the two antennas. At noon, this difference is zero. As the sun moves to the West, the signal will arrive at the West antenna a little earlier than East one. The delay depends on the "hour angle"*).
3. Now sketch the response we expect out of the interferometer for the period of 20 minutes around noon.
4. Bonus question: What happens when we observe at some time other than noon?

5 Coordinate Systems

Coordinate systems help us identify a position in 3D space. Each coordinate system is uniquely determined by the origin or reference point, the axes fixed with respect to the origin (3 coordinates) and the reference or preferred direction. For each Cartesian coordinate system, we can find an equivalent spherical coordinate system. Spherical polar coordinates are particularly useful for finding objects in the celestial sphere with the Earth as the origin.

Cartesian and Polar Coordinates

We define spherical polar coordinates to a point on the surface of the sphere as a radial distance from the origin, and two angles θ and ϕ defined as angles subtended between the z-axis and the equatorial XY plane (See Figure 18).

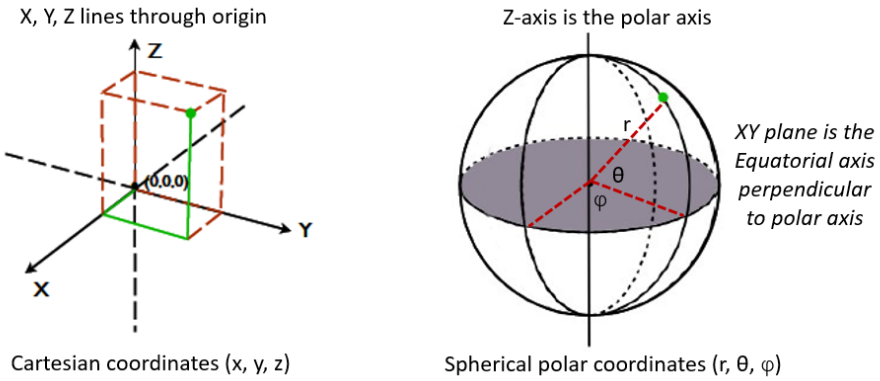

Figure 18: Cartesian and Spherical Polar Coordinates

We can define the (r, θ, ϕ) spherical polar coordinates in terms of X,Y and Z:

$$r^2 = X^2 + Y^2 + Z^2,$$
$$\tan\phi = Y/X,$$
$$\sin\theta = Z/R.$$

We can reverse this to get into Cartesian coordinates from Spherical polar coordinates such that:

$$X = r\cos\theta\cos\phi,$$
$$Y = r\cos\theta\sin\phi,$$
$$Z = r\sin\theta.$$

Coordinates on Earth

When establishing a coordinate system on the Earth, we take the origin to be the centre of the Earth. We use the Earths equator to define a reference plane - the Equatorial plane and we choose our reference Axis to be the rotational polar axis, which slices between the **geographical** North and South poles. The great circles which pass through the North and South poles are known as "meridians". The prime "meridian", or Greenwich Meridian, passes through the Royal Greenwich Observatory, London, United Kingdom. Great circles which lie parallel to the equator are known as parallels. On Earth, positions are usually given by two angles, the longitude and the latitude coordinates on the surface of the Earth (elevation).

Longitude and Latitude

The latitude is the angular distance north or south of the equator measured in degrees.

The Longitude is measured east or west as the angle between the reference meridian (the Greenwich meridian) and the meridian under consideration.

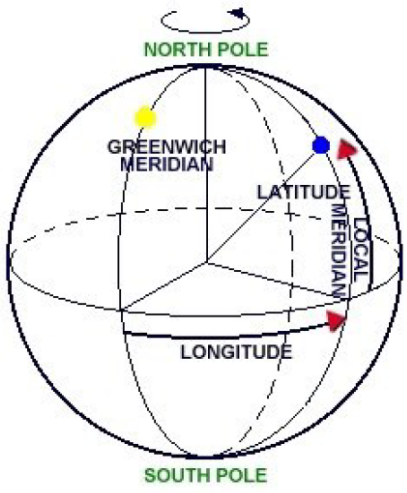

Figure 19: Longitude and Latitude definitions

Questions

What is the longitude and latitude of...
a) the Ghana Space Science and Technology Insitute (GSSTI)
b) the Hartebeesthoek Radio Astronomy Observatory (HartRAO)?

What other poles does the Earth have that could be confused with the geographic poles?

The Celestial Sphere

Compared to the size of the Earth, all celestial objects are far away. An observer can look at the skies as being manifested on the interior of a big (virtual) sphere - the Celestial Sphere. Each direction away from the observer will intersect the celestial sphere in one unique point, and thus positions of celestial objects can be measured on this virtual sphere.

Horizon System

There are a number of different systems for defining Celestial coordinates. First lets look at the Horizon System. This is defined locally for each observer on Earth and is based on the observers location. We define the area of the sky directly above us as the "zenith". We can then define our position in terms of Altitude and Azimuth.

Altitude and Azimuth

Altitude (or elevation) is the angle measured along a vertical circle from the horizon, it is measured in degrees. An alternative to altitude is the **zenith angle**, $z = 90° - \text{altitude}$.

Azimuth is generally defined as thee angle between the vertical through the star, measured eastwards from the north along the horizon from 0° to 360°. This definition applies to observers in both the northern and the southern hemispheres.

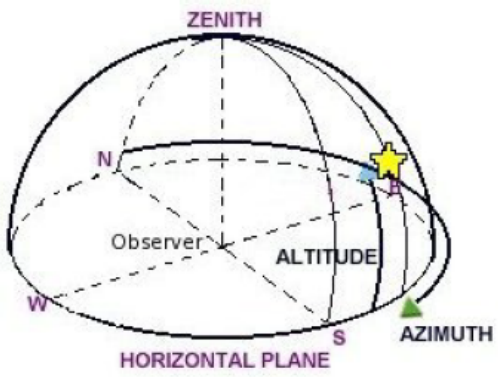

Figure 20: The Horizon System

Question

How close does the Sun come to the zenith at your current location? When does this occur?

Equatorial System

Since the elevation and altitude of a star are different for different places on the Earth, the horizon coordinate system is not useful for cataloguing celestial positions. A more useful coordinate system for locating celestial objects is one fixed at the celestial sphere. This is known as the **equatorial coordinate system**, we can imagine straight lines from the Earths centre produces the celestial equator and the north and south celestial poles. In this system we can define the declination and right ascension as being analogous to the latitude and longitude of the Earth. The coordinates are shown in Figure Figure 21. Also shown is the ecliptic, this is the path along which the Sun appears to move in the sky. Ecliptic coordinates are used for the positions of solar system objects, particularly the plants. Ecliptic Longitude and Latitude are measured in degrees.

Declination and Right Ascension

Declination (Dec. or δ) of a star is its angular distance in degrees measured from the celestial equator along the meridian through the star. It is measured north and south of the celestial equator. It ranges from 0° at the celestial equator to +90° at the North Celestial Pole (NCP) and -90° at the South Celestial Pole (SCP).

Right Ascension (RA. or α) is the angle between the meridians through "the first point in Ares" and a celestial object. "The first point of Ares" is the zero point given as the point at which the Sun cross the equator on March 21st (vernal equinox in the northern hemisphere and the autumnal equinox in the southern hemisphere). It is measured in units of time from 0^h to 24^h along the celestial equator eastwards (counter-clockwise)

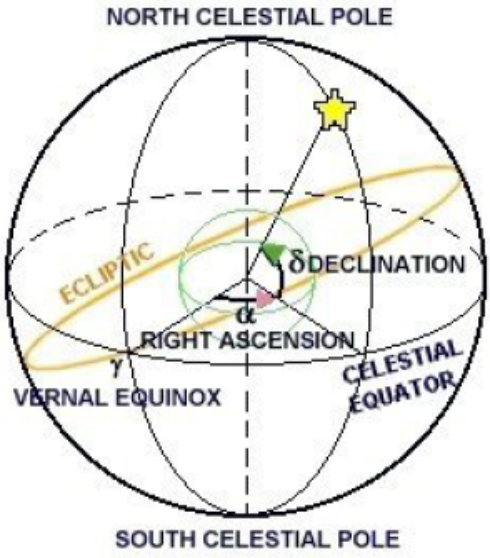

Figure 21: Celestial Coordinate System

Question

Why is the ecliptic titled? and by how much is it tilted?

Epoch, Precession

Having settled on Right Ascension and Declination as the natural coordinate system for most celestial objects, we find that the RA and Dec of celestial objects very inconveniently change with time. The reason for this is that the direction in which the Earth's axis points is changing, owing to the tidal pull on the not quite spherical Earth. This effect is called **Precession** (Figure As a result, an **Epoch**

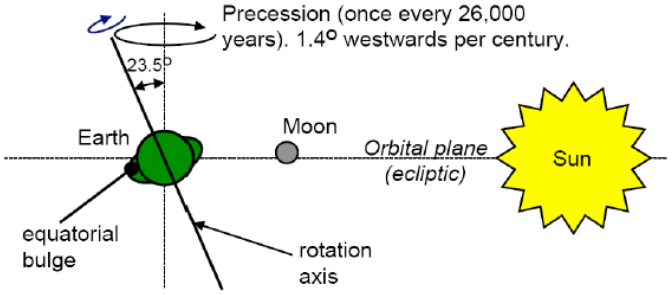

Figure 22: Precession of the Earth's axis

must be stated in respect of all RA, Dec coordinates. Standard epochs for catalogues of objects were B1900, B1950 and J2000. Here B stands for Besselian, and J for Julian, and describe subtle changes of definition.

To get the current position of an object in order to observe it, its coordinates must be precessed from the catalogue epoch to the date and time of observation. Generic Equatorial Coordinates are plotted on a rectangular in Figure 23.

Galactic Coordinates

For objects in the Milky Way, the **Galactic coordinate system** is also used. The direction of zero longitude and latitude is towards the centre of the Milky Way. This coordinate system does not vary with time, unlike RA, Dec. As an early attempt at defining the origin of the Galactic Coordinates was found later to be inaccurate, a second zero point was determined, and in this system Galactic longitude and latitude are called **Lii**, and **Bii** respectively and are shown in Figure 24. In Figure 25 we can see Galactic Coordinates mapped onto Equatorial coordinates (how we would see it from Earth), shown are both the Galactic centre and anti-centre.

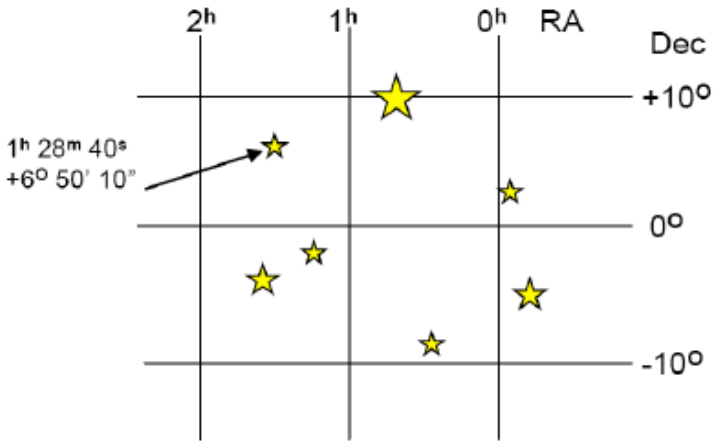

Figure 23: RA, Dec coordinate system

The Galactic centre and anti-centre

The centre of the Milky Way is around 7000 parsecs away. Towards Lii = 0°, Bii=0° lies Sagittarius A*, a compact radio source at J200 RA $17^h45^m37^s$, Dec 28° 56' 10". It passes over South Africa once per day.

The Galactic anti-centre direction at Lii = 180°, Bii=0° lies the well known constellation Orion at J200 RA $5^h45^m37^s$, Dec 28° 56' 10".

Radio emission from the sky is shown in equatorial coordinates in Figure26 and in Galactic coordinates in Figure 27. In the Southern hemisphere, the Galactic centre passes above the sky, in Figure 26, we can identify the Galactic centre by the brighter region with the visible spur, this is known as the North Polar Spur and is a region of sky with high levels of Synchrotron emission that are visible in radio wavelengths.

Time - Universal Time, Sidereal Time, Julian Date

Universal Time comes in more than one form. **Universal Time Coordinated (UTC)** is also known as **Greenwich Mean Time (GMT)**. It is the time measured by a evenly running clock positioned on the Greenwich Meridian. The world is divided into Time Zones: 15° change in longitude is an equivalent to an hour's change in time. One year is technicallt the Earth's **tropical period**. This is the time that elapses between two alignents of its axis of rotation with the Sun (or 365.242 days). The Earth's **orbital (sidereal) period** around the Sun is 365.256 days. The 0.014 day is equivalent to **20 minutes** and is caused by precession, which has a period of 25770 years.

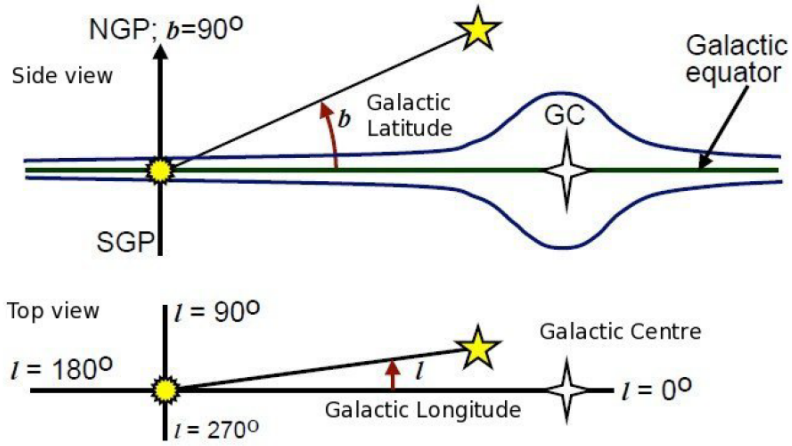

Figure 24: Galactic Coordinates - Latitude (Bii) and longitude (Lii).

Time Zones of DARA

Ghana Standard Time (GST) is on the same time longitude as Greenwich, so is in the Time Zone UTC + 0.

South Africa is roughly 30° East of Greenwich, so South African Standard Time (SAST) is set to be 2 hours ahead of UTC.

The Earth turns once on its axis in 23 hours 56 minutes and 04 seconds. This is called a **sidereal day**. Stars will rise ar the same time each sidereal day. However we set our watches to a length of day matching the mean **solar day**. The Earth has to turn for an extra 1° to get the Sun back to the same place in the sky, as it moves almost 1° per day in its orbit around the Sun. The length of the mean solar day is well known as 24 hours.

To point out telescopes we have to make allowance for the actual, irregular rotation period of the Earth. **UT1** is the time scaled used to measure this. **Leap seconds** are inserted in UTC at intervals to keep UTC and UT1 within 0.9 of a second. Measuring the changing length of day (UT1) is done by a global network of radio telescopes using quasars far out in the universe as fixed radio beacons. The HartRAO 26m telescope is part of this network.

A time scale divided into years with months of different lengths and numbers of days per month and year is very awkward when dealing with time series of data. To get around this the **Julian Date (JD)** was devised. This is the number of decimal days since 12h00 UT of January 1st, 1,4713 BCE. **Modified Julian Days (MJD)** are also used. They start at 0^h00 UT and are defined as:

$$\text{MJD} = \text{JD} - 240000.5 \tag{50}$$

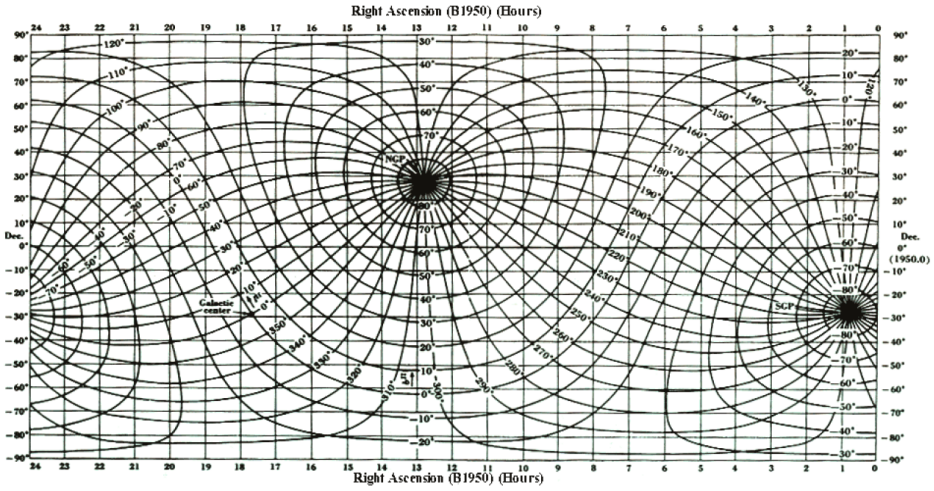

Figure 25: Galactic Coordinates mapped onto B1950 Equatorial coordinates.

Question

The Julian Date on 2009 August 5$^{\text{th}}$ at 10h00 UT was 2455048.875, what was the MJD?

Using Sidereal Time

As with all longitude-like coordinates, a zero point has to be set to sidereal time. This is the sidereal time at the Greenwich meridian, or **Greenwich Mean Sidereal Time (GMST)**. It is the elapsed time sinze the zenith meridian transit of the vernal equinox at the Greenwich meridian. **Local Mean Sidereal Time (LMST)** is then the current Greenwich Mean Sidereal Time plus the observer's longitude (East longitude is positive), converted from degrees to hours.

$$\text{LMST [h]} = \text{GMST [h]} + \text{Longitude}[^\circ/15] \tag{51}$$

A small correction (< 1.15 seconds of time) to this for **nutation** (18.6 year period wobble of Earth's pole) gives the **Local Apparent Sidereal Time (LAST)**. This equals the Right Ascension of all bodies currently crossing the observer's zenith meridian. Observatories often display clocks showing the Local Sidereal Time to aid observers. The **Hour Angle** of an object is the angle of an object East or West of the observers zenith meridian.

$$\text{HA} = \text{LST} - \text{RA}. \tag{52}$$

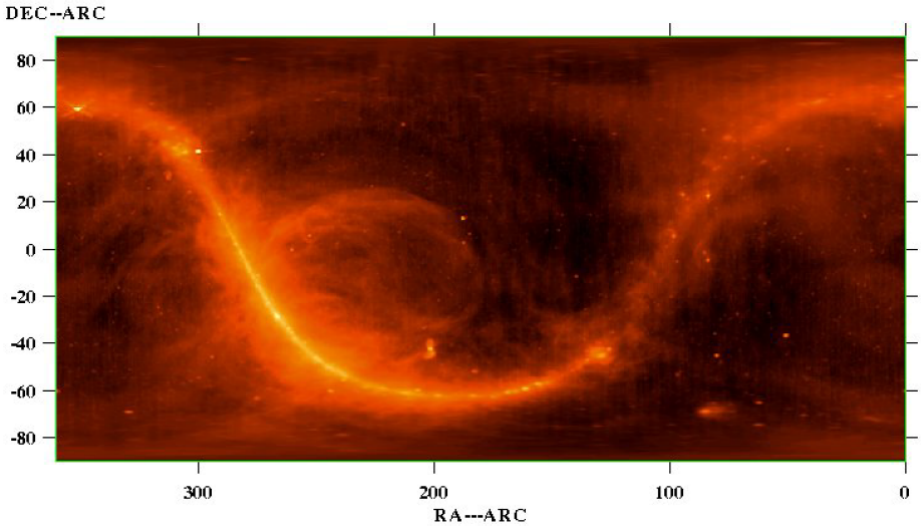

Figure 26: Radio sky at 408 MHz in J200 Equatorial coordinates (Haslam et al. 1982). Shown using rectangular projection with RA in degrees.

Hour Angle

A negative HA is the time until an object crosses the observers zenith meridian.

A positive HA is the time since the object crossed the observers zenith meridian.

Question

The LST in Johannesburg is $22^{\mathrm{h}}30^{\mathrm{m}}$. Where in the sky is 3C48, one of the radio Galaxies used for flux calibration, whose coordinates are approximately $01^{\mathrm{h}}34^{\mathrm{m}}$,+34°54”?

Refraction

Ground-based telescopes have to observe through the Earth's atmosphere. Refraction by the atmosphere increases the apparent elevation angle of an object. The effect is largest for objects close to the horizon (see Figure 28). Refraction by the atmosphere is greater by about 8% for radio waves compared to visible light. Refraction also depends on the hieght of the observatory above sea level and on the weater vapour content of the atmosphere. A simple approximation to the radio refraction is:

$$\Delta z = (n-1)\tan(z), \tag{53}$$

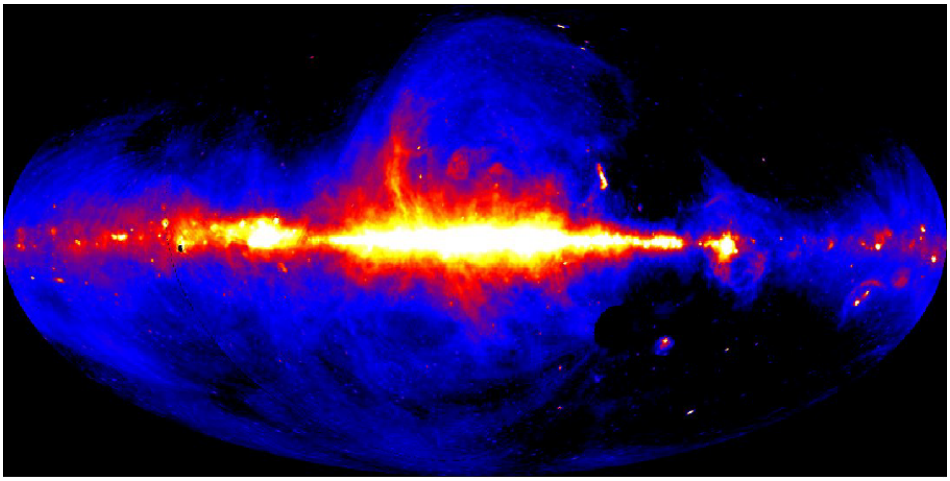

Figure 27: Radio sky at 2300 MHz in Galactic coordinates (Jonas et al. 1998). Left one-third from Stockert telescope, Germany. Right two0thirds from HartRAO 26m telescope. Shown using the Mollweide equal area projection.

where Δz (radians) is the apparent increase in elevation angle at zenith angle z (radians); n is the refractive index such that $n - 1 = 3 \times 10^{-4}$ for radio waves at sea level. Note that this refractive index changes with altitude. At Hartebeesthoek, at an altitude of 1400m, the refractive index $n - 1 = 2.5 \times 10^{-4}$ for radio waves.

Question

The horizon for the radio telescopes at Hartebeesthoek varies from 3° to 12° elevation as they are located in a valley. What is the approximate radio refraction in degrees at those two elevation angles?

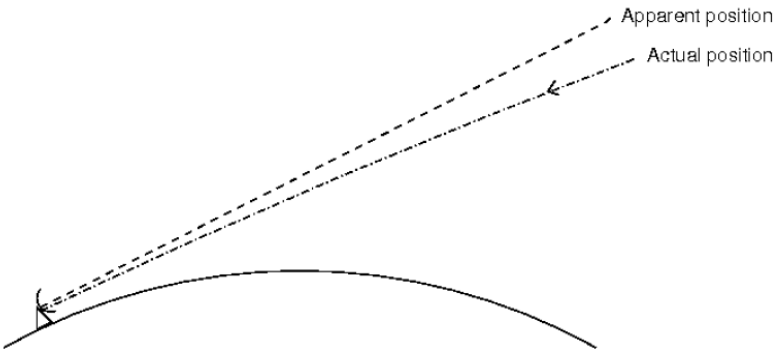

Figure 28: Diagram showing the change of refractive index with elevation.

Astronomical Distances

For relatively small astronomical distances, the **Astronomical Unit (AU)** can be used. This is defined as the mean Sun-Earth distance which is 149.6×10^6km (Figure 29). For large distances, the **Parsec (pc)** is used. This is defined as being equal to the distance from the Sun at which the mean Sun-Earth distance (1 AU) subtends an angle of 1 arc second (Figure 29). One parsec equals 3.086×10^{13}km, or 3.26 light years.

Figure 29: Definition of the Astronomical Unit and Parsec.

Parallax

A consequence of the Earth's motion around the Sun is that nearby objects in space appear to move forwards and backwards against the background of very distant objects, through **parallax** (See Figure 30). The amount of parallactic movement is proportional to their distance, so the observed parallax provides an absolute measure of their distance. Optically, this has long been used to measure the distance to nearby stars. We refer to the angle as the parallax angle, p (in arc seconds) and we can get the distance, d by;

$$d = 1/p \tag{54}$$

Parallax

Radio telescopes separated by thousands of kilometres can measure parallaxes of milliarcseconds (mas). These networks of radio telescopes are now being used to measure the distances to star-forming regions in the Milky Way, using the annual parallax of methanol and water vapour masers embedded in the star-forming clouds.

Question

The methanol masers in the star-forming region G9.62+0.20 were found by Sharmila Goedhart in her morning with the HartRAO telescope to show regular flaring, the first ever found in masers in a star-forming region. The parallax of the masers has been measured to be 0.194 mas. What is their distance?

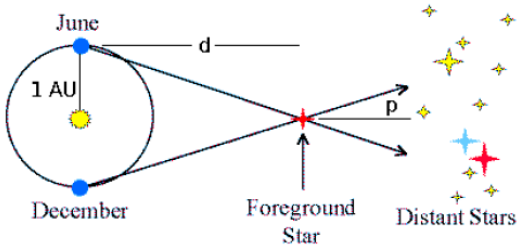

Figure 14: Parallax measurement

Figure 30: Parallax measurement

Astronomical Aberration

Telescopes are not fixed in space, they are on a moving Earth. As the speed of light is finite, this causes the apparent position of objects to shift. We have to point the telescope at the apparent position of the object to allow for this stellar aberration (Figure 31). Annual aberration was used by Bradley in 1727 to measure the speed of light.

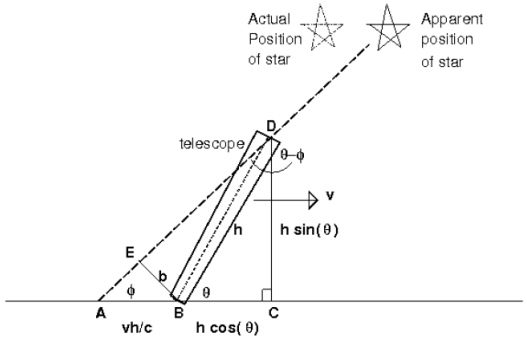

Figure 31: Stellar Aberration showing telescope pointing direction without aberration.

Solving for Stellar Aberration

Looking at Figure 31, we want to solve for the aberration angle $\theta - \phi$.

1. $\sin(\theta - \phi) = b/h$, where h is the height of the telescope tube and b is the line which subtends the line that marks the distance to the apparent position of the star.
2. $sin\phi = \frac{b}{vh/c}$, where v is the horizontal motion of the telescope owing to the Earths orbit and c is the speed of light (so h/c is the time taken for the light to travel down the telescope tube).
3. Rearrange for b, such that $b = \frac{vh}{c} \sin\phi$...
4. Now substitute for b to get $\sin(\theta - \phi) = \frac{vh}{c} \frac{\sin\phi}{/} h$...
5. So $\sin(\theta = \phi) = \frac{v}{c \sin\phi}$
6. For a small angle approximation, we can see that $\theta - \phi \approx \frac{v}{c \sin\phi}$.

Question

What is the constant of aberration in units of arc seconds for: a) The annual aberration caused by the Earth orbiting the Sun? b) The daily aberration, for the Earth turning on its own axis?

The International Celestial Reference Frame

To measure radio source positions and parallaxes accurately, reference sources with very accurately measured positions must be available. To create this reference frame, radio telescope networks have measured, and continue to measure, the positions of hundreds of quasars across the sky. This is called the **International Celestial Reference Frame (ICRF)**, shown in Figure 16. The HartRAO 26m telescope has played a key role in this project, being one of the few southern radio telescopes equipped for this. All the telescopes observe the same object at the same time, in a technique known as Very Long Baseline Interferometry (VLBI). Observations are made at two widely spaced frequencies (2.3 and 8.4 GHz) in order to measure and correct for the (varying) effects of the Earth's atmosphere and ionosphere. The networked radio telescopes are able to measure source positions to better than one milliarcsecond, whereas ground-based optical telescopes can achieve about 100 milli-arcseconds. As a result this extra precision, the radio source-based reference frame replaced the optical FK5 reference frame in 1998. The ICRF is crucial for comparing the positions of objects observed at different wavelengths across the electromagnetic spectrum, i.e. through multi-wavelength astronomy. In order to understand the relationship between the emission seen at different wavelengths, it is necessary to accurately align and overlay the images taken at each wavelength.

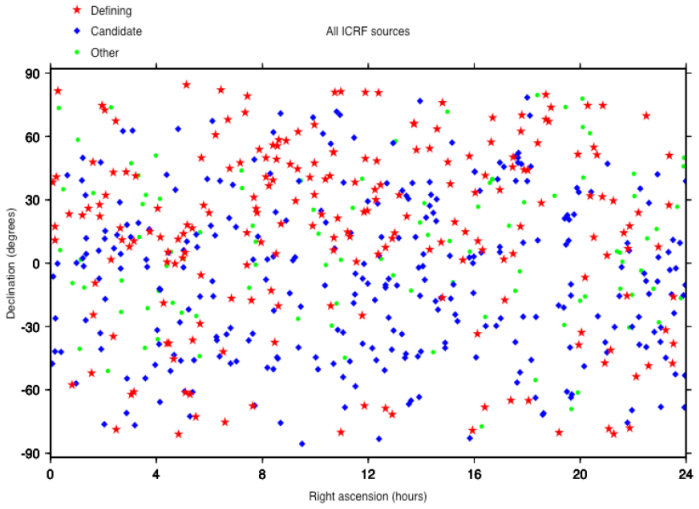

Figure 32: International Celestial Reference Frame

International Terrestrial Reference Frame (GNSS, SLR, DORIS)

At the same time as radio source positions are being measured precisely in the ICRF, so the positions of the participating radio telescopes are also determined with high precision. After taking out short-term effects such as tides in the solid Earth, we are left with long term motions of the radio telescopes (Figure 33), which measure the motion of the tectonic plates on which they are located (Figure 34). The accurate absolute positions of the these telescopes means that systems that measure relative positions can be co-located with them, and the absolute positions transferred to these systems. They include the Global Navigation Satellite Systems (GNSS) such as the US Global Positioning System (GPS), Russian GLONASS and European Galileo, Satellite Laser Ranging (SLR) and Doppler Orbitography and Radio positioning Integrated by Satellite (DORIS). These four systems are located at Hartebeesthoek, making it a key station in the International Terrestrial Reference Frame (ITRF). There are many scientific and practical spinoffs from the precise position measuring that these systems carry out.

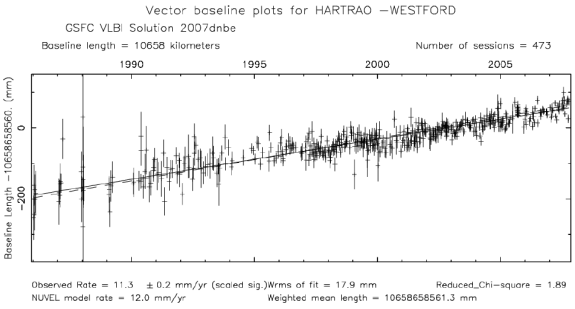

Figure 33: Changing distance between SA and USA

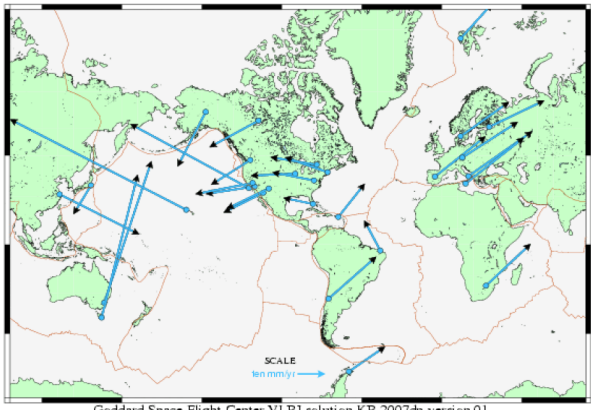

Figure 34: Radio telescope motion vectors

Question

What uses of high precision position measurement with GPS can you think of?

6 Digital Backends and Digital Signal Processing

This section provides supplementary material on Digital backends and Digital Signal Processing (DSP) techniques. To start this section we will look at what a digital backend is, explore hardware and software and then look at the mathematics and techniques required for processing a radio signal.

The backend of the receiver can be thought of as being the electronics and processing after the LNA. We can break this down into three parts, the Radio Frequency (RF) part with analogue electronics, the Intermediate Frequency (IF) part which down converts the electronics to frequencies that can be processed by the computer and finally the digital part of the back-end, this includes the digital processing and algorithms that must be applied to the signal in order to extract relevant information. We won't go into too much detail on the algorithms for DSP in this section, but we will cover the hardware and the basics.

Types of Radiometer

A radiometer is a way of measuring the total power of a signal. In radio astronomy, we are interested in signals that are weak compared to noise and in our receiver are very noisy components, such as the low noise amplifiers. Therefore we need a way of calibrating the gain in our receiver, and tracking it over time to make sure that we can separate out our signal from the noise. When talk about the different types of radiometer, we are talking about the different types of methods of gain calibration.

The most standard radiometer is a total power radiometer.

Down Conversion

A radio receiver takes an incoming radio frequency (RF) signal and converts it into bands that can be processed by the DBE. When we have to shift the frequency to do this, the receiver is super-heterodyne.

Digital Signal

Types of Noise

A radio receiver takes an incoming radio frequency (RF) signal and converts it into bands that can be processed by the DBE. When we have to shift the frequency to do this, the receiver is super-heterodyne.

7 Pulsars

Pulsars are unique astrophysical tools for testing fundamental laws of physics. Using pulsars we can test theories of gravity, extremes of matter, magnetic and electric fields and dynamics. They can even tell us much about the early universe and merging black holes!

First, we need to understand "What is a pulsar?". A pulsar is a rotating neutron star found in the remnant of supernovae (SNe). Pulsars are mainly radio emitters and emit in narrow beams. They have a clock like stability in their rotation. Essentially, pulsars are rapidly -rotating Cosmic Radio Lighthouses. Most normal pulsars spin down and die after a few million years when their periods reach 1-8 seconds.

Typical Pulsar Properties

- Mass $M = 1.4M_{\odot}$
- Radius $R = 10km$
- Period $P = 0.0013 - 8.5$s
- Magnetic Field Strength $B = 10^8 - 10^{14}G$

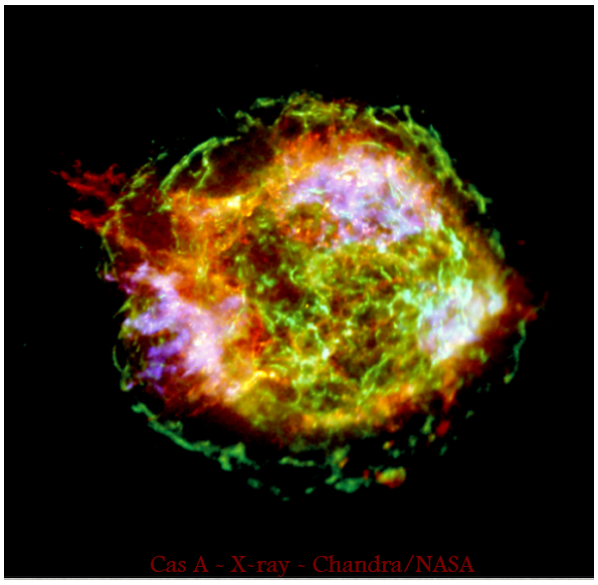

Figure 35: The CasA pulsar, part of the Crab Nebula supernova remnant (SNR).

Pulsar Rotation

The pulsar spin is due to the conservation of angular momentum from a star that was spinning before it exploded. The nature of the pulse comes from the structure of the magnetic field, creating a magnetic dipole. The simplest model of a pulsar magnetosphere is the Goldreich-Julian model (P. Goldreich and W. H. Julian, ApJ, 157, 869, 1969). This states that *"In spite of its intense surface gravity, the star must possess a dense magnetosphere. The particles in the region threaded by those field lines which close within the light cylinder rotate with the star"* and that *"In the co-rotating zone, the space-charge is the component of magnetic field parallel to the rotation axis. The field lines which extend beyond the light cylinder close in a boundary zone near the supernova shell. Charged particles escape along these lines and are electrostatically accelerated."* It's these accelerated particles that create the **radio beam**.

What does a pulsar sound like?

PSR B0329+54 has a period of $P = 0.71452s$, that's 84 revolutions per minute

PSR B0833-45 has a period of $P = 0.089s$, that's 674 revolutions per minute

PSR B0531+21 has a period of $P = 0.033s$, that's 1800 revolutions per minute

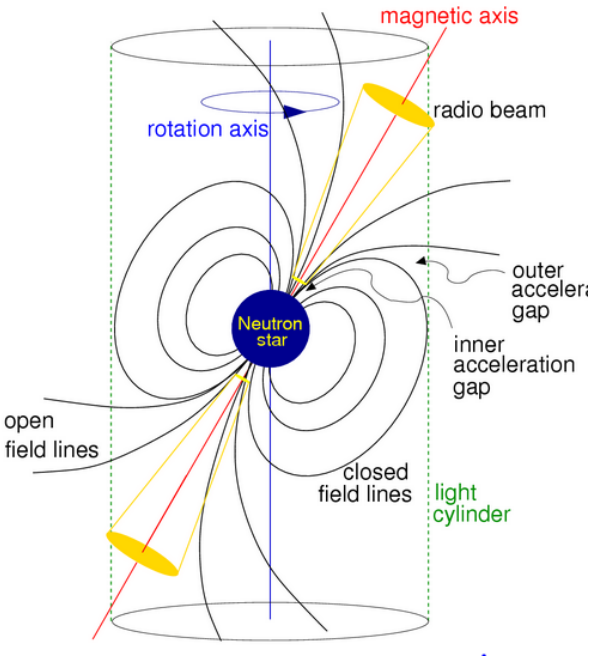

Figure 36: Pulsar Mechanisms - showing how pulsar winds can escape the magnetic field, results in an emission cone.

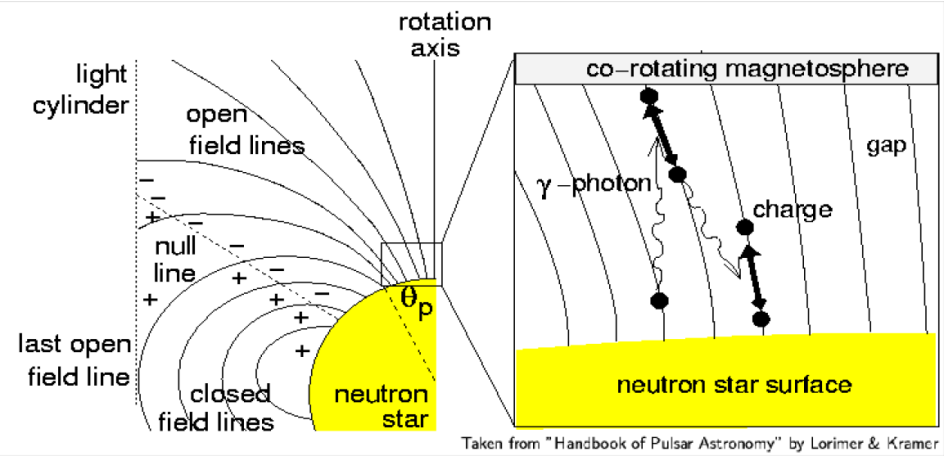

Figure 37: Diagram showing the open and closed field lines and the movement of photons and charged particles close to the neutron star surface.

The P-Pdot diagram

A P-P dot diagram is a graph that plots the rotation period of pulsars with the rate of change in their periods. The aim is to reveal patterns that can tell us the characteristics and evolution of pulsars. Generlly, a pulsars period will slowly lengthen over time, although sometimes a pulsar will jump to a shorter period, most likely due to a 'pulsar quake' where the internal mass of the pulsar shifts. The P-P dot diagram tens to show a difference between binary pulsars and lone pulsars, where the binary pulsars have a shorter period and don't slow their rotation as quickly.

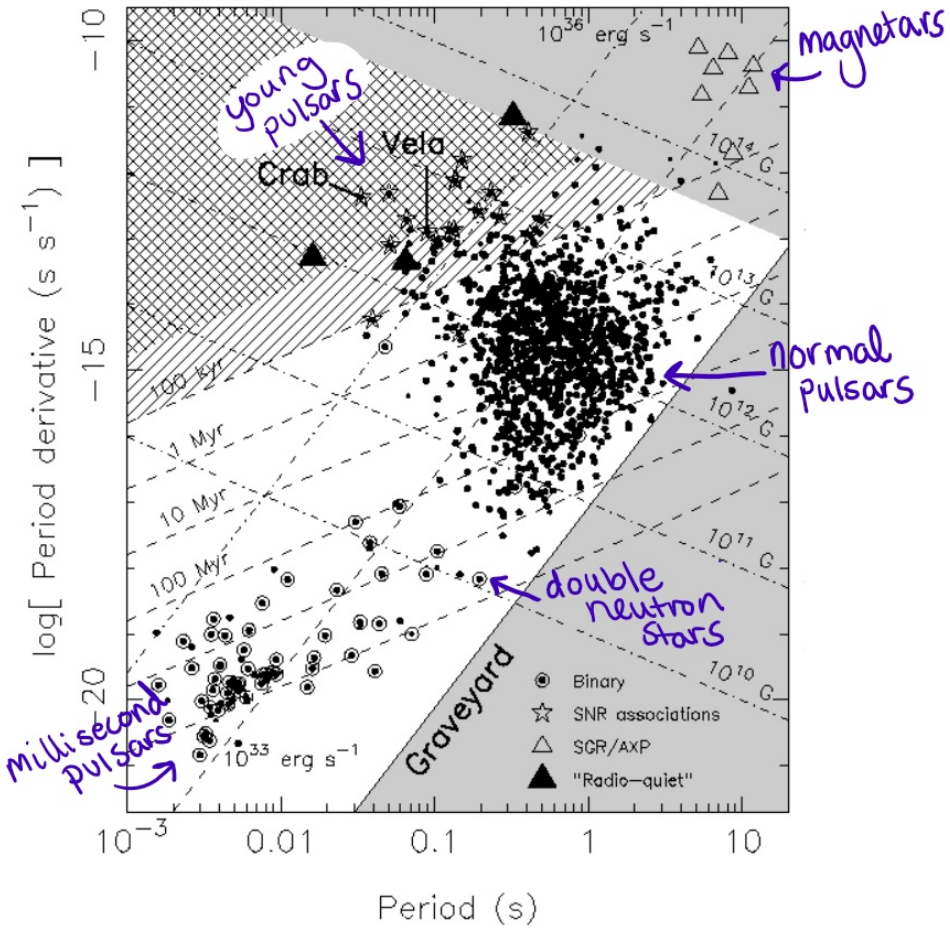

Figure 38: P-P dot diagram taken from "Handbook of Pulsar Astronomy" by Lorimer & Kramer. Labelled with the typical locations of different types of pulsars.

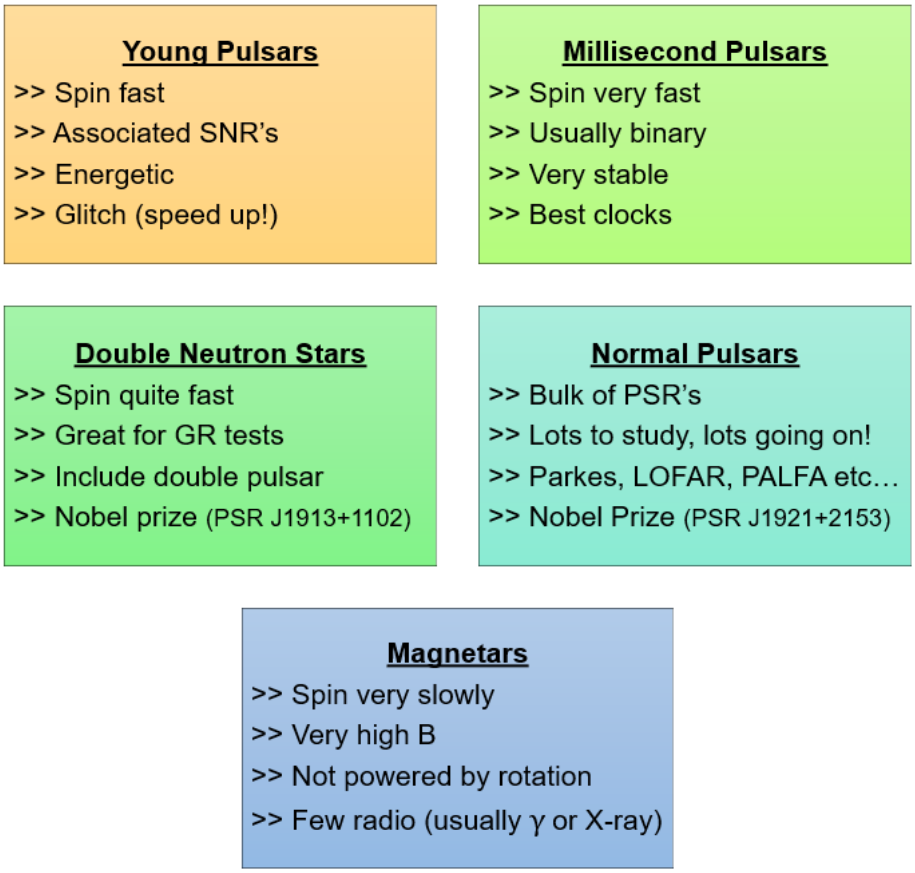

Figure 39: Overview of pulsar types and characteristics.

Pulse Phenomenology

[H] The nature of a pulsar pulse isn't always straightforward. The study of pulse phenomenology looks at the differences in types of pulse and pulse profiles. First lets look at the types of pulses. **Giant pulses** appear as high energy spikes with a very short duration, there can also also be small sub-pulses that create **micro-structures** in the pulse profile. Finally, **spiky** pulses can have two types of profile, broad and weak or narrow and bright.

We can break down pulse intensity variations into three types. Firstly, Rotating radio transients (**RRATs)** these are sources of short, moderately bright, radio pulses, typically rotating magnetised neutron stars, which emit more sporadically often with higher pulse-to-pulse variability than most typical pulsars. When a pulsar "turns off" for a period of time, we refer to these as being **Nullers**, it is the sub-pulses that keep the phase. There are also intermittent pulsars that can be off or on for un-predictable periods of time.

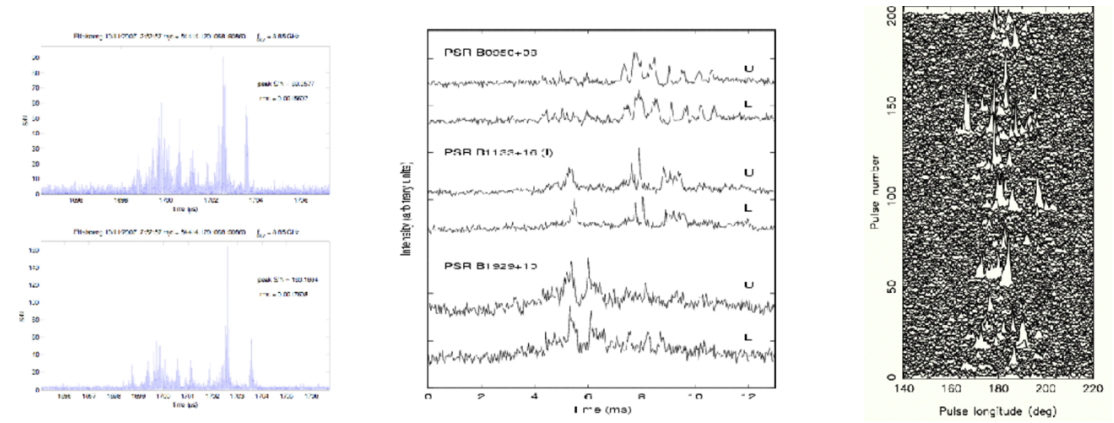

Giant Pulses	Microstructure	Spiky
• Handful of sources • Associated with high energy • 100's-1000's > average • Duration <2ns!	• Make up the sub-pulses • Not seen in all pulsars • Some quasi-periodic • Emission element?	• Two classes of pulses • Some broad and weak • Others are narrow and bright • Explains some RRATs

Figure 40: Types of Pulse - Note the emission element of micro-structure pulses, this means that they may arise from additional emission mechanisms.

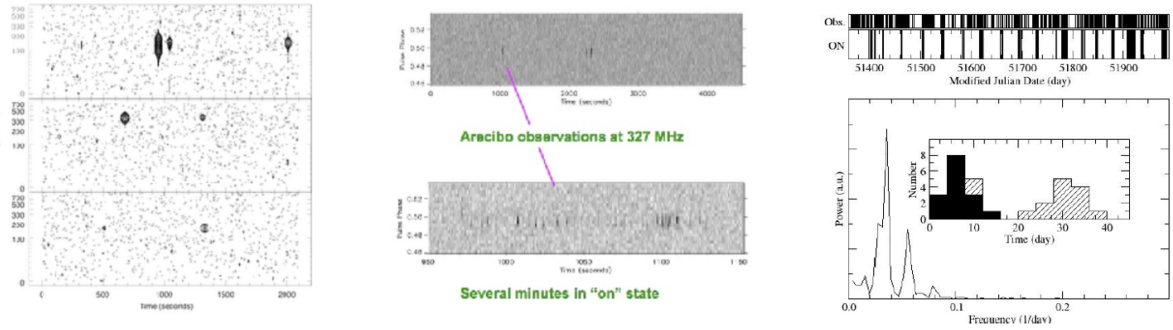

RRATs	Nullers	Intermittent
• Only see single pulses • Rates of <few/hr • Total on time sec/day • PSR like P and Pdot	• Off for 1 pulse to hours • Pulses come in groups • Sub-pulses keep phase • More extreme version	• On for days – months • Off for days – months • Quasi-periodic?

Figure 41: Intensity variations in pulsars.

Lovell Timing Database

The Lovell Telescope is located at the Jodrell Bank Observatory in the north West of England. It's main use is the continuous monitoring of pulsars. The Lovell Timing Database is a unique program for monitoring the rotational properties of more than 700 pulsars, including more than 70 millisecond pulsars. More pulsars are being added all the time as new surveys reveal new sources. The longest time span is now 40 years for the Crab pulsar, with an equivalent of 400 pulsars with a span of ¿ 10 years. The observations are made on timescales ranging from daily to monthly, but generally are taken about 1/20 days on average. This results in ¿ 9000 years of rotational history! This allows the studies of timing noise, profile evolution, glitches, binary systems, monitoring interstellar medium, tests of gravity and even the search for gravitational waves!

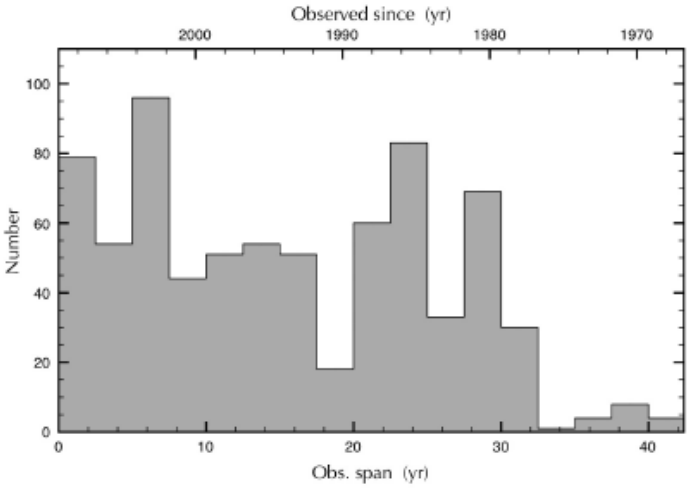

Figure 42: Lovell Timing Database

The Best Clocks

The large moment of intertia means that pulsars are like giant flywheels and thus are very stable rotators. For very bright pulsars we can measure the arrival time of the pulse to a few nanoseconds. Pulsars rival the best atomic clocks here on Earth. This makes them excellent for studying GR (see GR section!).

Period of Second Fastest Pulsar

P = 1.5578064924327±0.0.0000000000004 milliseconds The best pulsars are predictable it 3 parts in 1,000,000,000,000,000, i.e. they keep time to 1 second in 30 million years!

8 Near Field Antenna Measurement

This practical shows us how to make a measurement of the near field of an antenna. First of all, we need to understand the difference between near and far field measurements. In the lecture notes we've seen a lot to do with far field beam patterns, this is the distance at which the magnetic and electric fields are strongest and can be detected separately. This has lots of useful applications, particularly in imaging (such as near field probes). In the far field radiation pattern, we're seeing a combination of the E and H fields, these are described by Maxwells equations. In Figure 43, we can see the definition of near-field, far field and the transition, or Fresnel zone.

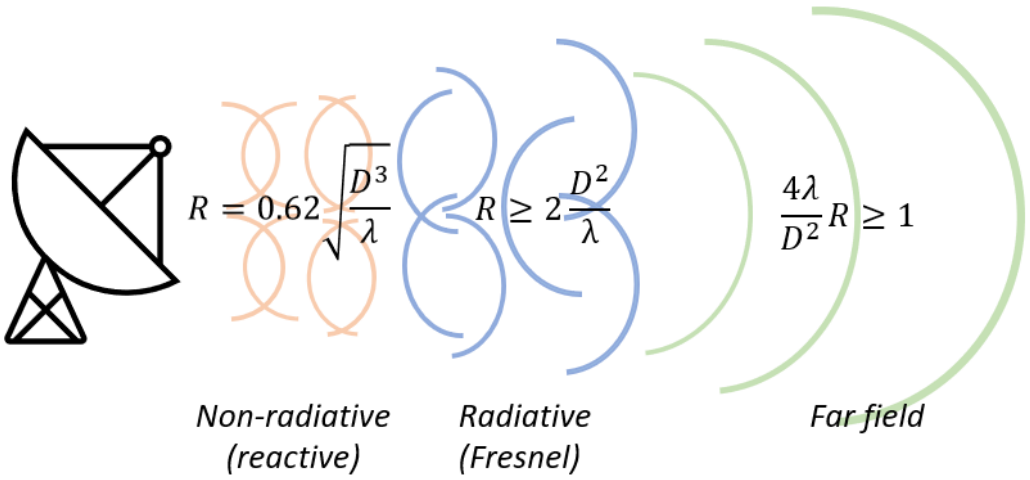

Figure 43: Diagram showing the distances for an antenna of diameter, D, in the near field, the Fresnel zone and the Far field of the beam.

Objective

To measure the radiation field from a 12 GHz horn antenna in the vicinity of a 12 GHz DSTV offset paraboloid antenna.

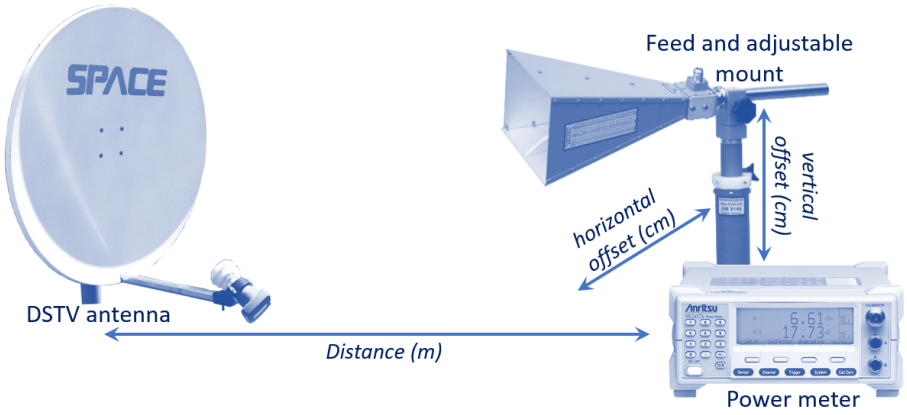

Figure 44: Example DSTV dish and power meter set up.

Method

1. The antennas are mounted on a support frame in an open area and connected to a microwave frequency synthesizer, with a clear line of sight along the line at which measurements will be made. The synthesizer is set to a frequency of **11 GHz** and a radiated power output of **+ 10 dBm**
2. A mobile measurement trolley is fitted with a small monitoring antenna and carries a **microwave power meter** to measure the received signal radiated from the antenna.
3. The measurement trolley is positioned at increasing fixed distances from the radiating antenna and a series of power measurements made with various heights of the monitoring antenna.
4. The received power is measured in **decibels (dB)** relative to 1 milliWatt ($10^{-}3$ Watt).
5. Record the measurements on a spreadsheet in the format noted in Figure
6. Use your power measurements to generate a series of plots to show how the received power varies as a function of height and distance from the radiating antenna.

Unit 2/3 DARA Training Program- Antenna near field tests

Distance	Vertical/Horizontal Offset (cm)										
(metres)	-100	-80	-60	-40	-20	0	20	40	60	80	100

Figure 45: Antenna near field measurement results table

Conclusions

1. What conclusions can be drawn from the results?
2. How does the measured field from the small horn antenna vary? Does it follow the expected inverse square law of distance from the transmitting antenna
3. How does the measured field from the dish antenna vary? Does it follow the expected inverse square law of distance from the transmitting antenna
4. Can you explain the difference between the two sets of measurements
5. Calculate the near field distance for the 26m antenna at wavelengths of 6 cm and 3.5 cm. *Hint: The Near field radiation pattern (the Freznel zone) extends for D^2/λ, where D is the linear dimension of the antenna aperture.*

9 Brightness Temperature of the Sun

In this practical, we will obtain an estimate of the brightness temperature of the sun at both 4 GHz and 12 GHz. We will be using a pinhole camera to calibrate the experiment, we will use a Digital Satellite Television (DSTV) dishes to make measurements at 12 GHz, and a mesh dish to measure the brightness temperature at 4 GHz. The brightness of the sun

A schematic of the DSTV apparatus is shown in Figure 46.

Objectives

1. Calculate the angular diameter of the Sun from your measurements from the pinhole projection. *Estimate the uncertainty (error) in your answers.*
2. Use your measurements with the DSTV dish to calculate the brightness temperature of the Sun at 12 GHz. *Estimate the uncertainty (error) in your answers.*
3. Use your measurements with the mesh dish to calculate the brightness temperature of the Sun at 4 GHz. *Estimate the uncertainty (error) in your answers.*

Angular Size and the Sun's Brightness Temperature

The difference between physical diameter and angular diameter depends on both the size of the object and its distance from us (see Figure 3). We see the Sun and the Moon as more or less the same size on the sky, this is because even though the Sun is 400 times the size of the Moon, it is also 400 times further away. As the projection of the antenna beam onto the sky is two-dimensional, we shall need to find the angular area that it covers. Angular area is called a "solid angle" and the units are radians^2, or steradians (sr). An object with an angular radius θ radians subtends a solid angle:

$$\Omega = 2\pi(1 - \cos\theta) \qquad [\text{sr}].$$

For small θ,

$$\Omega = \pi\theta^2 \qquad [\text{sr}].$$

We can use this equation to calculate the solid angle of the Sun as seen form the Earth, Ω_s.

The beam solid angle Ω_A of the antenna can be obtained from the half-power beamwidth (HPBW) in units of radians by assuming the main lobe of the beam has a Gaussian shape:

$$\Omega_A \approx 1.133(\text{HPBW})^2 \qquad [\text{sr}].$$

The Sun's brightness temperature T_B can then be estimated by scaling its measured antenna temperature T_A by the ratio of the beam solid angle Ω_A to the Sun's solid angle Ω_s, and correcting for the

main beam efficiency ϵ_m being less than unity:

$$T_B = \frac{\Omega_A T_A}{\Omega_s \epsilon_m}$$

Detecting Radio Emission from Space

When the telescope looks at a radio source in the sky, the receiver output is the sum of the radio waves receiver from several different sources:

- Behind the radio source whose brightness we want to measure is the cosmic microwave background (CMB) coming from every direction in space. This is the radiation emitted as the first atoms formed, 380 000 years after the Big Bang. The black body temperature of the CMB Tcmb has now decreased to 2.7 Kelvins, as the expansion of the Universe has stretched out the waves by a factor of 1000. The CMB produces a brightness temperature T_{Bcmb} of $\approx$ 2.7 K at 1.4 or 4 GHz, reducing to 2.5 K at 12 GHz.
- The emission from the radio source we want to measure, which produces the antenna temperature T_A.
- Radiation from the dry atmosphere T_{at} and from the water vapour in the atmosphere T_{wv}. The dry air adds about 1K, and at 12 GHz water vapour adds 1 - 2 K, depending on the humidity.
- The radiation the feed receives through the antenna sidelobes from the (warm $\approx$ 290 K) ground or nearby buildings beyond the edge of the antenna, of brightness temperature T_g. With the antenna pointing straight up at zenith this could add 5 - 15 K; 10 K is a reasonable number to use. It increases when pointing close to the horizon.
- The amplifiers in the receiver generate their own electronic noise and so produce a receiver noise temperature T_R.

The sum of these parts is called the "system temperature" T_{sys}. Summing from the most distant noise contributor to the nearest we have:

$$T_{sys} = T_{Bcmb} + T_A + T_{at} + T_{wv} + T_g + T_R \qquad [\text{K}]$$

Apparatus

The main parts of a simple radio telescope comprising of a satellite dish and radiometer are shown in Figure 46. The incoming radio waves from natural emitters are weak and noise-like. If the output of the detector is connected to a loudspeaker, the signal sounds like a hiss, as one hears if a radio is tuned off-station. The internal noise produced in the amplifiers is generally larger than the signal from natural radio sources.

Calibrating the Radio Telescope

You will need two pieces of card, a pencil, a sharp knife, a rule and a 2 metre tape measure.

The satellite dish produces an output voltage proportional to the temperature of the object it is pointed at plus its own internal receiver temperature. We need to establish a scale of Kelvins per radiometer output unit. We do this by using the sky at zenith as a "cold load", and the ground as a "hot load". If V_1 and V_2 are the two meter reading and c is a constant of proportionality, then:

$$T_R + T_{sky} = cV_1 \qquad [\mathrm{K}] \tag{55}$$

where $T_{sky} = T_{Bcmb} + T_{at} + T_{wv} + T_g \approx 15\mathrm{K}$.

$$T_R + T_{ground} = cV_2 \qquad [\mathrm{K}] \tag{56}$$

We can estimate T_{ground} by touch or measure it using an infrared detector. We can use equations 55 and 56 to solve for the two unknowns, c and T_R.

Measure the Antenna Temperature from the Sun

We need to aim the telescope at the Sun. With an offset-fed paraboloid this can be a little tricky. Hold the dish horizontal. then turn the dish horizontally so the shadow of the feed arm falls across the centre of the dish. Then rotate the dish in elevation so the shadow of the feed arm on the dish gets shorter. The Sun comes into the beam just after the shadow leaves the edge of the dish. Adjust the direction gently up and down and sideways to maximise the signal from the Sun; the signal should roughly double. Take a new meter reading V_3:

$$T_R + T_{sky} + T_{Asun} = cV_3 \qquad [\mathrm{K}]. \tag{57}$$

As c and T_R are known from the calibration, and we have a reasonable estimate of T_{sky}, we can immediately calculate the antenna temperature of the Sun as measured with this telescope using Equation 57.

Next we need to measure the angular diameter of the Sun and of the telescope beam in order to calculate the solid angles they subtend.

Measure the Angular Diameter of the Sun

The usual sources of information will give the angular diameter of the Sun. However we can actually measure for ourselves the angular diameter of the photosphere - the surface of the Sun from which light is emitted. Use pinhole projection to measure the angular diameter of the Sun. On one piece of

card use a ruler and pencil to mark three equilateral triangles several cm apart, with sides of about two, three and four millimetres. Cut out the triangles using the sharp knife and ruler.

The card with the holes is used to project images of the Sun onto the second card (Figure 47). The two cards need to be separated by a distance D, measured by tape measure. The linear diameter d of the projected Sun is measured with the ruler. The angular diameter of the Sun is d/D radians, so its angular radius Θ_s is given by:

$$\Theta_s = \frac{d}{2D} \tag{58}$$

From its solar radius Θ_s, calculate the solid angle subtended by the Sun Ω_s.

To optimise your experiment:

- What shape should the projected Sun have?
- Which hole gives the best image to work with?
- What distance D (large or small) will give the most accurate result?

Measure the Half-Power Beamwidth of the Radio Telescope

The half-power beam width (HPBW) of the antenna can be estimated using

$$\text{HPBW} = \text{FWHM} \approx 1.2\lambda/D \qquad \text{[radians]}.$$

If the satellite dish is mounted on a tripod or mount so that it can be locked in position, then it is possible to carry out a "drift-scan£ across the Sun.

Point the antenna to get the maximum signal from the Sun. Lock the antenna's position. Immediately write down the time (minutes and seconds) and the voltage on the meter recording the signal strength, and repeat every ten seconds.

The drift scan will give a cross-section of half the antenna beam pattern. The time for the signal to go from maximum to halfway down to minimum is equal to half of the HPBW, in seconds. Units of time are converted to angle by noting that the Sun moves through 1 degree in 4 minutes/cosine(Sun's declination).

The Sun's declination is how far north or south of the equator it is at the time of observation. Get the "Apparent Dec" of the Sun for the measurement date from *http://www.calsky.com/cs.cgi/Sun/1?*

Calculate the Brightness Temperature of the Sun

We now have the Sun's solid angle Ω_s from $\Omega_s = \pi\theta^2$, the beam solid angle Ω_A and the antenna temperature measured from the Sun T_A. We can now calculate the brightness temperature of the Sun:

$$T_{Bsun} = \frac{\Omega_A T_A}{\Omega_s \epsilon_m} \qquad \text{[K]}. \tag{59}$$

What we are missing Equation 59 is a value for the main beam efficiency, ϵ_m. Experiments indicate that a reasonable value for ϵ_m for a DSTV dish at 12 GHz is about 0.75. For mesh surface satellite dishes working at 3.8 GHz, a lower value is more likely as the surface shape is less accurate, so ϵ_m is about 0.5. For a mesh dish with a 1.4 GHz can feed, ϵ_m is about 0.5. These values are based on measurements with domestic satellite dishes.

Questions

- Estiamte the uncertainty in your result in the usual way, by propagating estimates of the error in each of your measurements. Assume an uncertainty in ϵ_m of 10%.
- How does the 4GHz measurement compare with the brightness temperature for the Sun measured at 12 GHz?
- How does your result for the Sun's brightness temperature compare to the temperature usually quoted for the Sun's photosphere (light emitting surface)? What do you think this implies?

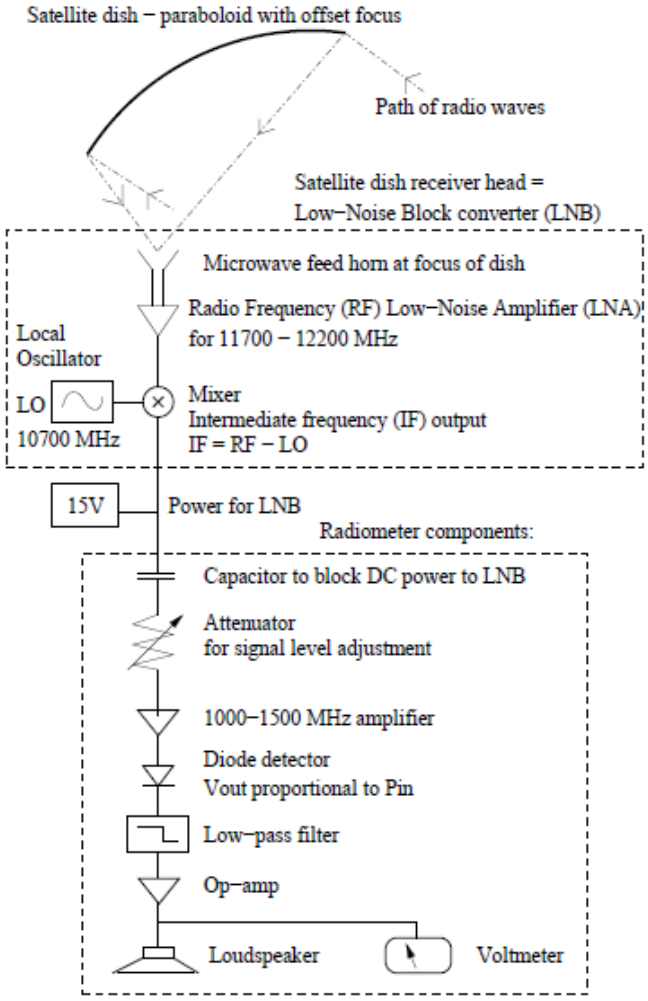

Figure 46: Block Diagram of 12 GHz Satellite Antenna and Radiometer.

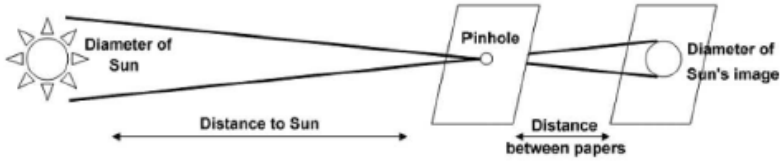

Figure 47: Sun projection schematic

10 LNA Calibration

In this practical we're going to cover how to calibrate an LNA. This is a useful exercise that will get you used to the idea of temperature control, gain and reading a spectrum analyzer. As explained in the Microwave Receiver lecture, a **hot** and a **cold** load are connected alternately to the amplifier input. The respective power that is transferred to the **Square Law Detector** is given by:

$$P_{out} = Gk(T_{\text{load}} + T_{\text{LNA}})B \tag{60}$$

The ratio of $P_{\text{hot}}/P_{\text{cold}}$ which is usually denoted by Y, reduces to:

$$Y = \frac{T_{\text{hot}} + T_{\text{LNA}}}{T_{\text{cold}} + T_{\text{LNA}}} \tag{61}$$

We can rearrange to get the LNA temperature:

$$T_{\text{LNA}} = \frac{T_{\text{load}} + YT_{\text{LNA}})}{Y - 1} \tag{62}$$

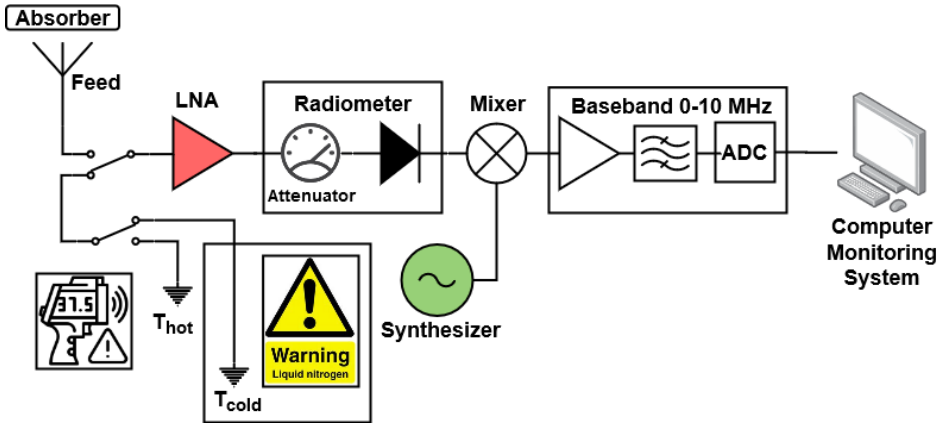

Figure 48: Schematic of the LNA calibration practical

Objective

To calibrate the noise temperature of a low noise amplifier using thermal reference terminations and to measure the system when the amplifier is connected to a horn pointed at the sky.

Equipment

1. A 7 GHz **low noise amplifier** attached to a test plate and connected to two waveguide switches which can connect to either of two reference thermal terminations or a horn antenna pointing at the sky
2. A room temperature termination (hot load)
3. A liquid nitrogen cooled termination (cold load)
4. A microwave absorber that can be placed in front of the feed horn
5. A total power radiometer incorporating a square law detector to measure noise powers
6. A microwave synthesizer to provide local oscillator to convert from 7 GHz to baseband, or 0–10 MHz in this case
7. An infrared thermometer for measuring the temperature of thermal loads
8. A microwave noise diode which provides a secondary calibration source
9. A computer monitoring system to record the radiometer
10. Necessary cables to connect the various modules together
11. DC power supply to power the radiometer

A hot and cold load are connected alternatively to the amplifier input. The respective power that is transferred to the Square Law Detector is given by:

$$P_{out} = Gk(T_{\text{load}} + T_{\text{LNA}})B \tag{63}$$

The ratio of $P_{\text{hot}}/P_{\text{cold}}$ which is denoted by Y reduces to:

$$Y = \frac{(T_{\text{hot}} + T_{\text{LNA}})}{T_{\text{cold}} + T_{\text{LNA}}} \tag{64}$$

rearranging for T_{LNA}

$$T_{\text{LNA}} = \frac{T_{\text{hot}} - YT_{\text{cold}}}{Y - 1} \tag{65}$$

Method

1. The equipment should be connected as shown in the diagram
2. Set the synthesizer frequency to 7.0 GHz, 10 dBm power level and note these values on the data sheet

3. Using the waveguide switch, select the liquid nitrogen (**cold load**) note that the meter reading should remain about 500 mV (Why?)
4. The instructor will start running the computer monitoring system
5. The instructor will then assist in filling the cold load with liquid nitrogen, observing all necessary safety precautions (e.g. use of protective gloves and a transparent face protector)
6. As the liquid nitrogen cools the load, the readings on the radiometer output meter and the computer monitor should decrease (Why?)
7. Once the temperature of the nitrogen load has stabilised the calibration can begin
8. Increase the 10dB step attenuator to 100 dB and record the radiometer output meter reading to get the correction bias
9. Return to the original attenuator setting (the radiometer output meter should read $\sim$ 500mV)
10. Record the meter reading, P_{cold}, averaging the range of fluctuations, if necessary
11. Switch to the **hot load**
12. Record the meter reading P_{hot}, averaging over the range of fluctuations, if necessary
13. Switch back to the hot load and charge the attenuator by +1dB, and repeat steps 15-16
14. Switch back to the hot load and change the attenuator by -2dB, and repeat steps 15-16

Analysis

Use the Y-factor formula to calculate the noise temperature. Note that the boiling point of liquid nitrogen has to be corrected for altitude, and frequency dependent correction made for which information will be supplied.

Measurements with Horn on Sky

1. Move the trolley with equipment outside onto the measurement platform
2. Check that the cold load has sufficient liquid nitrogen, and top up if necessary
3. Switch the waveguide switches so that the horn is connected to the sky
4. Increase the 10 dB step attenuator to 100 dB and record the radiometer output meter reading to get the correction bias
5. Return to the original attenuator setting prior to step 4
6. Record the meter reading P_{sky} averaging over the range of fluctuations if necessary
7. Place the absorber foam over the feed

8. Record the meter reading P_{absorber} averaging over the range of fluctuations, if necessary
9. Use the **infrared thermometer** to measure the physical temperature of the absorber material and record
10. Remove the absorber from the feed and change the attenuator by +1 dB, and repeat steps 6-8
11. Remove the absorber from the feed and change the attenuator by -2dB and repeat steps 6-8

Analysis of horn results

There is a simple formula for calibrating these results:

$$T_{\text{sys}} = \frac{T_{\text{absorber}} + T_{\text{LNA}}}{Y} \tag{66}$$

where $Y = T_{\text{absorber}}/T_{\text{sky}}$ For T_{LNA} use the average of the three measurements calculated in the calibration stage.

Notes on temperature of cold load

The physical temperature of the cold load is determined by the boiling point of liquid nitrogen, 77.3 K at standard pressure. At 5 GHz, the additional loss between the load and the output connector introduces additional noise, **increasing T_{cold} to 82.5 K** At altitude the boiling point **decreases by 0.3 K per 300 m** altitude

11 Spectroscopy Data Reduction

In this experiment we will see how obtain spectra from our data by carrying out bandpass corrections and applying a pointing correction factor. For HartRAO, long-term monitoring is used and so point source sensitivity (PSS) is determined by an average value after being observed over a long time period.

Instructions

1. Load and plot the data
2. If **pointing offset observations have been done**
   (a) do bandpass correction
   (b) measure the amplitude at the offset positions
   (c) calculate the pointing correction factor assuming a Gaussian beam
3. Do bandpass correction on frequency-switched on-source pairs
4. If more than one pair of observations have been done, repeat previous step on each pair
5. Apply pointing correction factor to on-source spectra
6. Apply point source sensitivity conversion factor for each polarisation (See Drift Scan Exercise)
7. Create an average spectrum for multiple observations for each polarisation
8. Add together **RCP** and **LCP** to get total intensity
9. Write the final spectrum to disk

Python Script

In this exercise you will be using a pre-written python script, when looking through the python script, remind yourself of how we open **FITS** files and how to read in both data from the **FITS** file and header information. For example, reading in the LCP and RCP data:

```
'LCP'   : hdulist[2].data['Polstate1'],\n",
'RCP'   : hdulist[2].data['Polstate4'],\n",
```

We also see that the header contains information on the pointing, beam size and bandwidth, all important information for reducing the correct data.

```
'units' : hdulist[2].header['TUNIT2'],\n",
'pointing' : hdulist[0].header['SPPOINT'],\n",
'position' : hdulist[2].header['POSITION'], \n",
'HPBW' : hdulist[1].header['HPBW'],\n",
'date' : hdulist[0].header['DATE-OBS'],\n",
'object' : hdulist[0].header['OBJECT'],\n",
'longitude' : hdulist[0].header['LONGITUD'],\n",
'latitude' : hdulist[0].header['LATITUDE'],\n",
'Focus' : hdulist[0].header['FOCUS'],\n",
'equinox' : hdulist[0].header['EQUINOX'],\n",
'bw' : hdulist[0].header['SPBW'],\n",
'nchan' : hdulist[0].header['SPCHAN'],\n",
't_int' : hdulist[0].header['SPTIME'],\n",
'fs_offset' : hdulist[0].header['SPFS'],\n",
'spVlsr' : hdulist[0].header['SPVLSR'],\n",
'restfreq' : hdulist[0].header['RESTFREQ'],\n",
'centrefreq' : hdulist[2].header['CENTFREQ'], \n"
'Tsys_lcp' : hdulist[3].header['TSYS1'],\n",
'DTsys_lcp' : hdulist[3].header['TSYSERR1'],\n",
'Tsys_rcp' : hdulist[3].header['TSYS2'],\n",
'DTsys_rcp': hdulist[3].header['TSYSERR2'] }\n",
```

Bandpass

The spectrum produced after the signal passed through a bandpass filter. The drop of the signal on the sides is due to the filter response. The filter acts as a square law detector, but it is not perfect. As you can see, the noise level for LCP and RCP is different. The noise level of the LCP and RCP is the antenna temperature.

Averaged bandpass corrections

To do the pointing correction we average the LCP and RCP. This will calculate the average of LCP and RCP and subtract that value from the entire spectrum and pull down the spectrum to zero level.

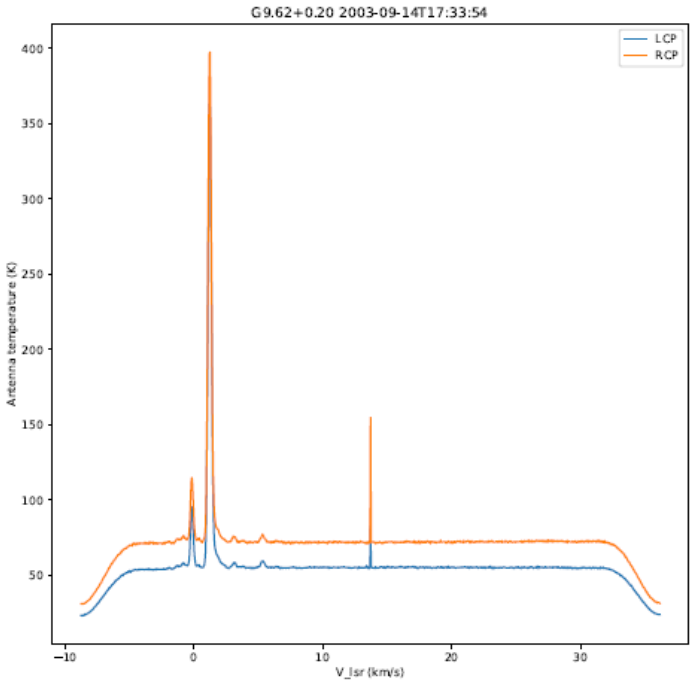

Figure 49: Bandpass of a 1 MHz filter at 6.668 GHz

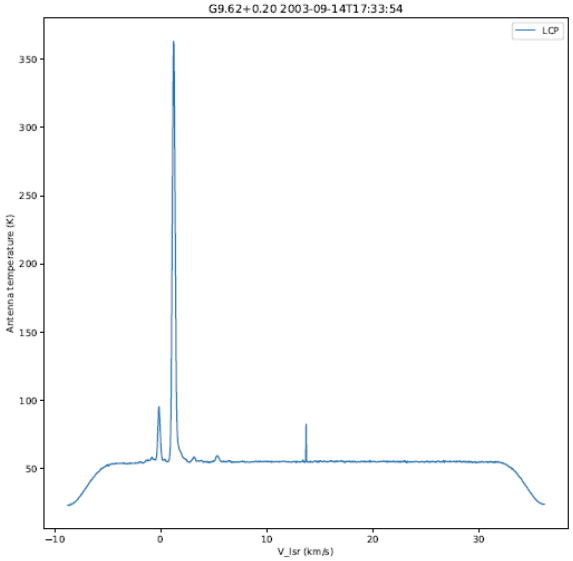

(a) First observation of a frequency switched pair

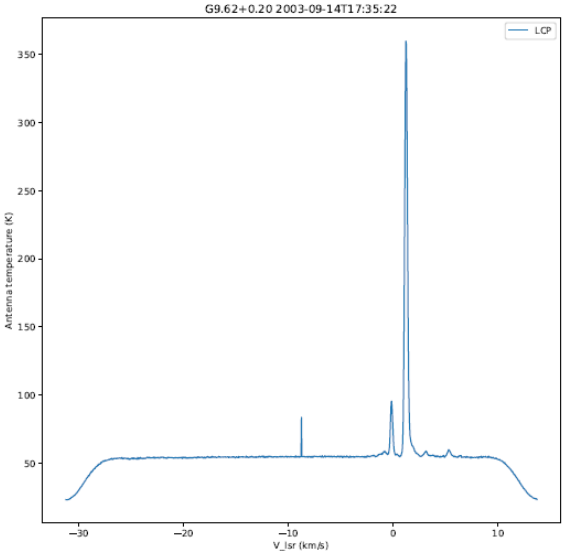

(b) Second observation of a frequency switched pair

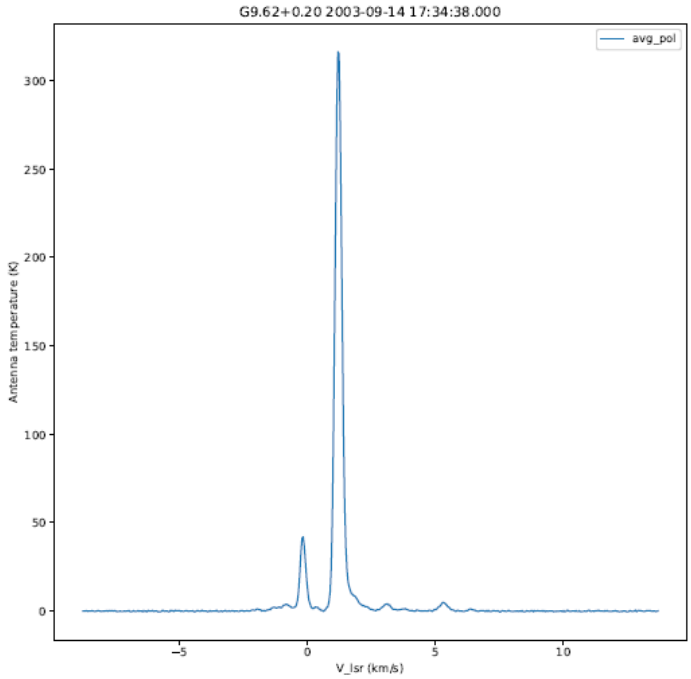

Figure 51: Averaged and bandpass corrected spectrum.

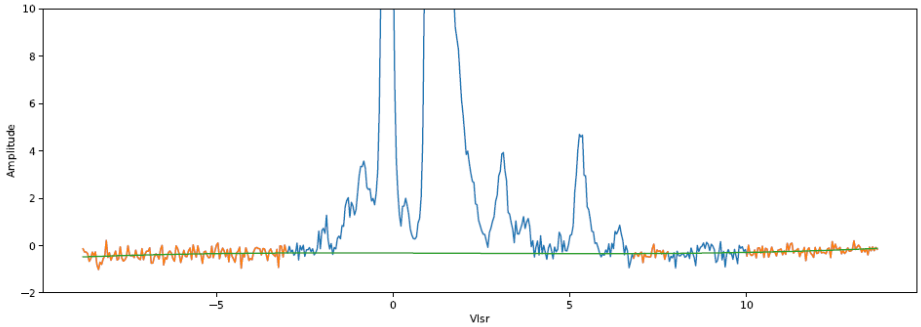

Figure 52: Chosen blocks for the baseline to flatten the baseline if necessary

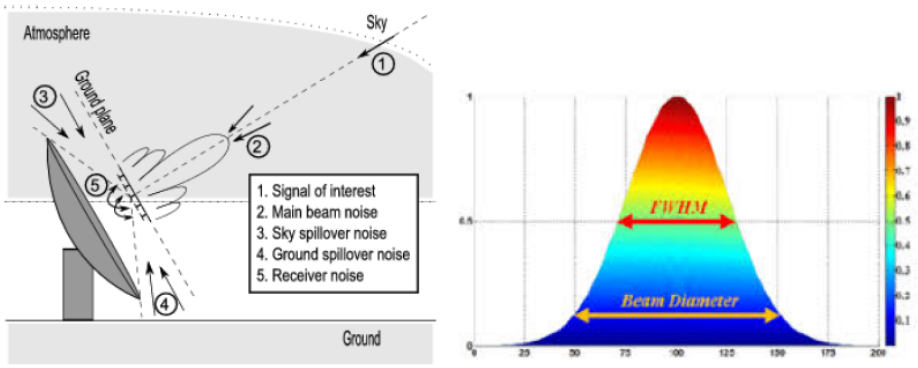

Figure 53: Antenna power distribution

Pointing Observations

Seen the power distribution of the main beam.

If we assume that the astronomical source emits spherical symmetrically, the power will be a Gaussian profile in the direction of the observer (in the case of the HartRAO telescope). To observe the maximum power from the source, the telescope must be pointed precisely on the source.

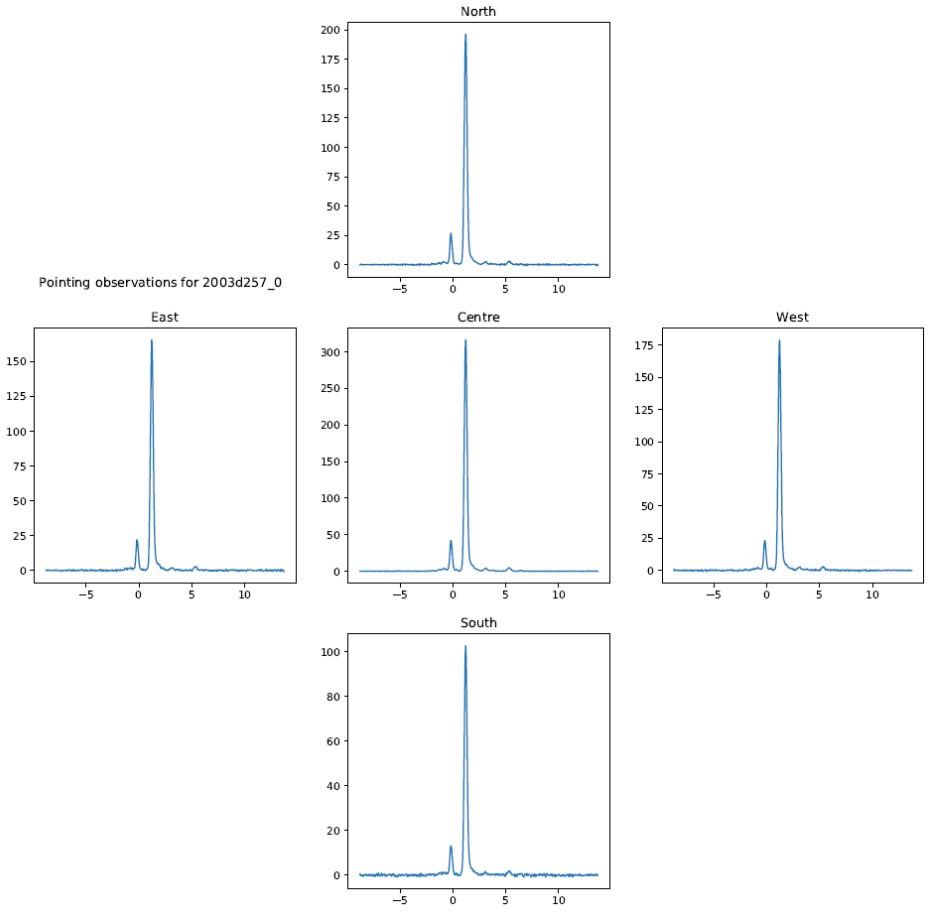

Figure 54: North, South, East, West and Centre pointing observations

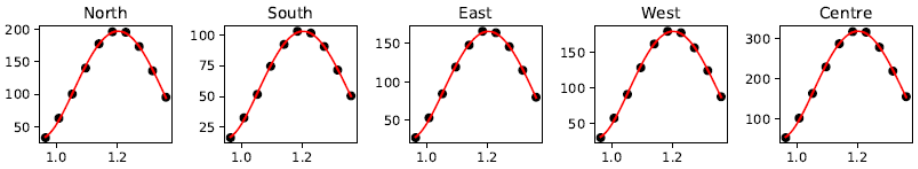

Figure 55: Gaussian fitting to each pointing observation to get the peak flux for each pointing

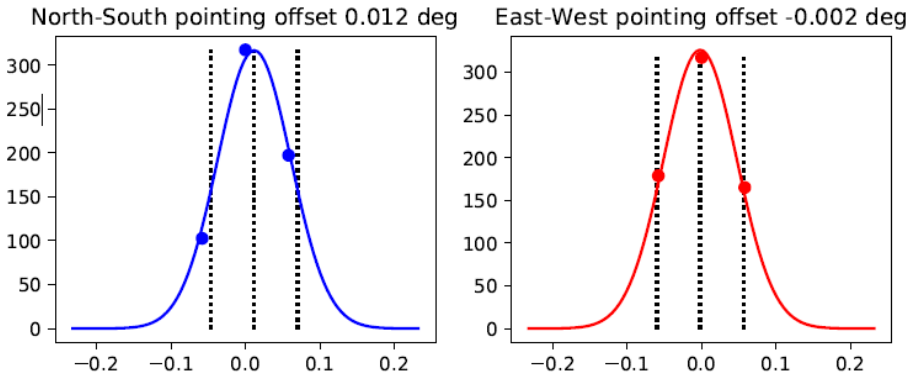

Figure 56: Gaussian fitted to the North-South and East-West pairs to calculate a possible off-set in each of these directions

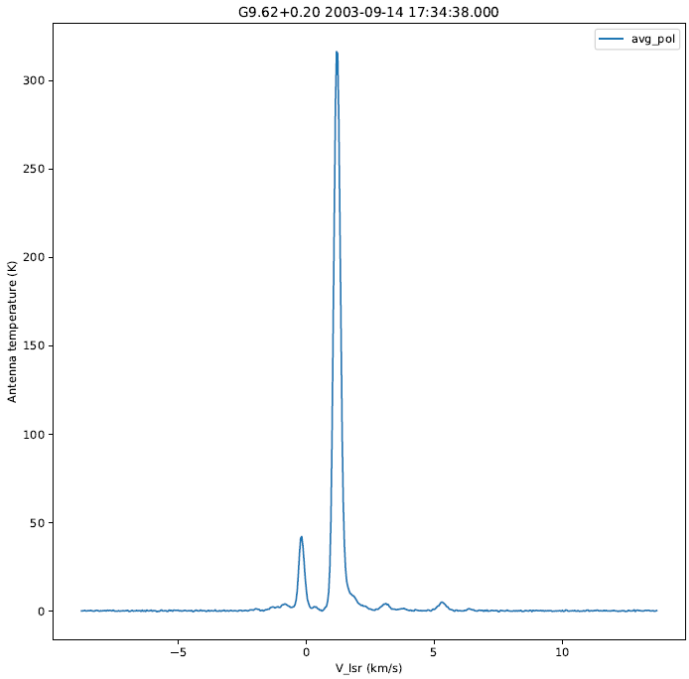

Figure 57: The final spectrum which is corrected for pointing correction factor

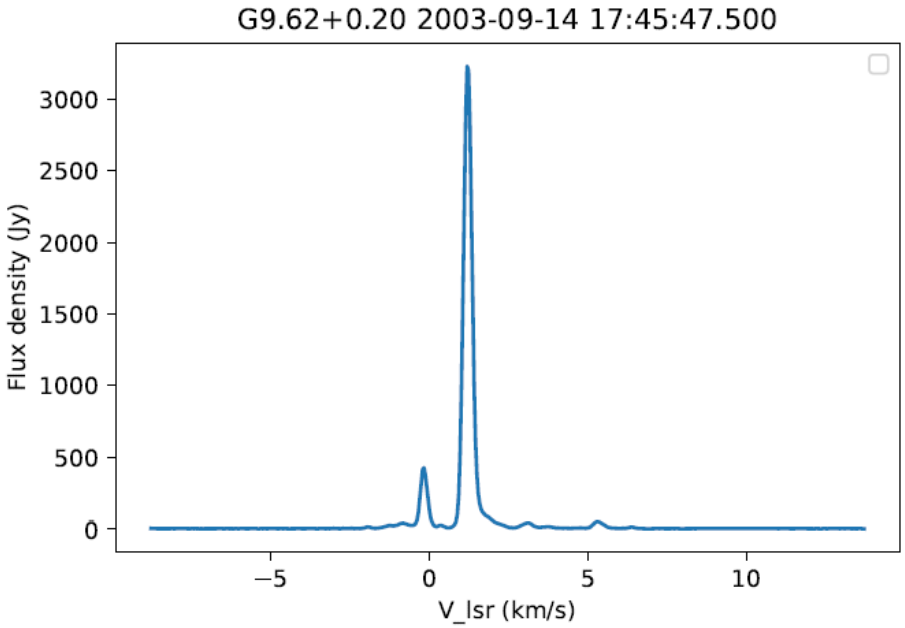

Figure 58: The final spectrum in flux density (Jy) after the spectrum is multiplied by the PSS which was determined from the Drift-scans

12 Drift Scan Exercise Questions

These questions are part of the follow up exercise of the Drift Scan observations tutorial found in `https://github.com/Pfesi/AVN_continuum_tutorial/blob/master/AVN_2019_Drift_scan_continuum_tutorial.ipynb`.

1. **Continuum Flux Measurement Calibration using drift scans of a calibrator, Hydra A at 4800 MHz, 8280 MHz and at 12218 MHz**

   (a) Measure the height of the peak emission in the centre above a line drawn through the minima on either side of the centre. Estimate the error. Do both left circular polarisation (LCP) and right circular polarisation (RCP).

   (b) Measure the full width at half maximum (FWHM = HPBW) and estimate the uncertainty for both LCP and RCP.

   (c) Compare to the HPBW calculated as $1.2\lambda/D_{antenna}$. Remember to allow for the apparent width of the beam RA = width of beam on sky/cos(decclination of source).

   > **Note**
   >
   > The FWHM of the telescope beam depends on the frequency of observation and the diameter of the dish, and therefore the FWHM of the telescope beam will decrease with increasing frequency. However, the width of the scan pattern is the FWHM of the telescope beam divided by the cosine of the declination of the source at the epoch of observation, as scans in Right Ascension are broadened by the secant of the declination of the source.

   (d) Calculate the effective area of the antenna and its aperture efficiency at 4800 MHz, 8280 MHz and at 12218 MHz (with uncertainties) from the Hydra A drift scans.

   > **Note**
   >
   > Ott estimate the Hydra A flux density at 4800 MHz to be 13.5 Jy, at 8280 MHz, it is 8.2 Jy and at 12218 MHz, it is 5.7 Jy. To find aperature efficiency we can use the equation:
   >
   > $$\eta_A = \frac{A_{eff}}{A_{phys}} = \frac{G\lambda^2}{4\pi A_{phys}}$$

   (e) Calculate how many Jy of flux density gives 1K of antenna temperature in each polarization at all frequencies, with uncertainties. This is called the **point source sensitivity** (PSS).

2. **Drift scans of quasar J1427-4206 at 4800 MHz, 8280 MHz and at 12218 MHz continuum flux density determination.**

   (a) Measure the height of the peak emission in the centre above a line drawn through the minima on either side of the centre. Estimate the uncertainty for both LCP and RCP.

   (b) From the PSS from Hydra A at each wavelength, calculate the flux density of J1427-4206 at each frequency, with error estimates.